DRFC/CAD

EUR - CEA - FC - 1447

Quasi-optical concepts for Lower Hybrid Waves Launchers on large Tokamaks

Ph. BIBET , J.P. CRENN

janvier 1992

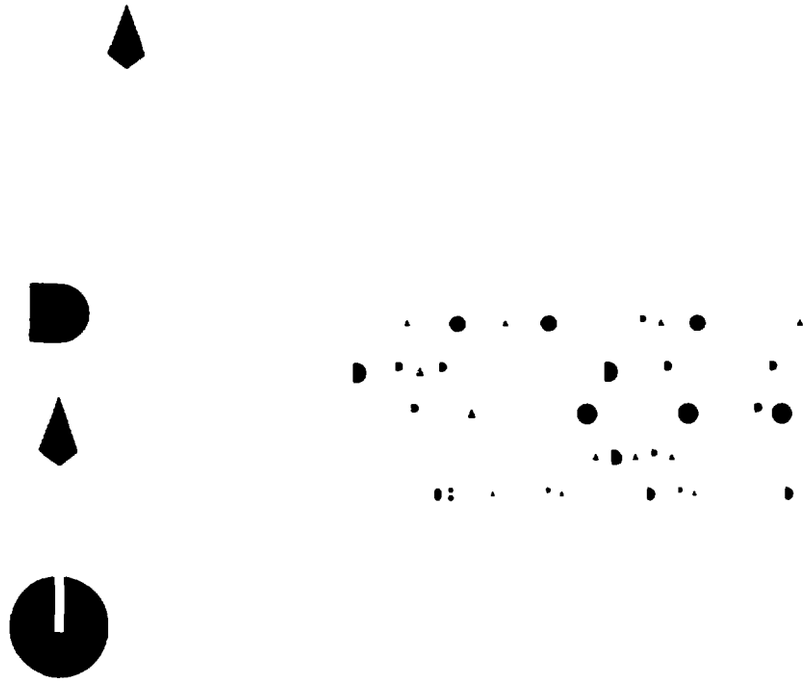

QUASI-OPTICAL CONCEPTS FOR LOWER HYBRID WAVES LAUNCHERS ON LARGE TOKAMAKS

Ph. BIBET, J.P. CRENN

Janvier 1992

RESUME

De nouveaux types d'antennes, utilisant des montages quasi-optiques, sont envisagés pour les futures expériences de chauffage et de génération de courant, à la fréquence hybride inférieure, sur les grands Tokamaks (JET, ITER). L'utilisation de techniques quasi-optiques dans ces antennes, présente un certain nombre d'avantages, permettant de concurrencer les techniques de guides d'ondes employées jusqu'à maintenant.

Dans le présent rapport, différents schémas quasi-optiques, associés à un Grill composé soit d'un réseau de guides d'ondes, soit d'un réseau de barreaux de diffraction, sont étudiés. Le calcul montre que l'utilisation d'un Grill en guides d'ondes conduit à des transmissions trop faibles, tandis que le Grill avec barreaux de diffraction ouvre des perspectives intéressantes. Ce dernier cas constitue donc l'axe de recherche souhaitable, mais les études déjà menées sont encore préliminaires et doivent être approfondies pour valider ou non les solutions envisagées.

CONTENTS

I - INTRODUCTION

Quasi-optical concepts for Lower Hybrid Waves (LHW) launchers on large Tokamaks (JET, ITER) have been recently envisaged [1] [2]. By comparison to the classical waveguide-grill type launcher, these new concepts must be better suited to large experimental devices, with high reliability during a long lifetime, simple and flexible mechanical structure, high power capability, good power transmission and efficient coupling to the plasma...

Different quasi-optical schemes are considered in this report and their ability to work well are evaluated and discussed. All these schemes are based on an optical transmission, with/without focussing mirrors, between Radiating Antennas (RA) and the Grill, which couples the beam to the plasma.

Two basic types of LHW launchers are taken into account :

1 - The Radiating Antennas and the Grill are composed of rectangular waveguides carrying the fundamental TE_{10} mode.

2 - The Radiating Antennas launch Gaussian beams and the Grill is made of optical rod arrays.

The present work aims at determining some devices of interest for which further calculations and improved conceptual design would be justified. Accordingly, this work has to be considered as a preliminary study, eliminating what looks like low-capability devices and, inversely, yielding some schemes and directions of research.

II - BASIC CONCEPTS WITH RECTANGULAR WAVEGUIDES IN THE RADIATING ANTENNA (RA) AND THE GRILL

II a - Description

A basic scheme, simply composed of an array of rectangular guides for the RA, and an other array of rectangular guides for the Grill is shown in Fig. 1. The fundamental TE_{10} mode is the one-mode propagating in the RA waveguides. In order to get an efficient power transmission, the radiated field from RA must be well directive, and the coupling between the incident wave on the Grill and the TE_{10} mode of each guide must be strong.

The device is surrounded by an absorbing wall, in order to avoid microwave power leakage outside. Vacuum would be set inside, making easier the handling of large beam power in the guides and in free-space.

This device cannot be assumed to work as a cavity with a pattern of reflected waves between RA and the Grill, because it would lead to very low Q values, and, without well defined modes.

Actually, it works like a transmission system with some microwave absorption and stray reflections. The field polarization keep quasi constant in the transmission, as the TE_{10} mode and then the free-space beam have a well defined linear polarization. In the present vacuum conditions, the field breakdowns would be avoided. The wave phase has to be adjusted inside the guides and the Grill, which would not be difficult to do. The main problem arising from this concept is the power transmission efficiency, related to the geometry of the device, the radiated beam directivity and the coupling of the incident power to the TE_{10} mode in each Grill waveguide.

II b - Theoretical aspects

The following calculations aim at determining the transmission of the beam power from the RA output to the TE_{10} mode in the Grill waveguides. Some assumptions and approximations are made:

- The waveguides of the RA have all the same rectangular geometry and size. The TE_{10} mode is the only one propagating in the guides, and unless it is expressed (Dolph-Tchebycheff method for instance), the amplitude and phase are the same in all the output apertures.

- The wave impinging the Grill is a plane wave with an uniform field distribution at each entrance of the waveguides.

- The Grill waveguides have all the same rectangular geometry and size.

- The faces of the Grill and RA are plane and parallel.

- The free-space medium is non absorbing and the stray reflections from the walls, the Grill and the RA are negligible.

- The Grill is located in the far-field of the RA. This condition is required in order to have simple calculations of the field pattern, but one must emphasizes that it is very constraining for an efficient power transmission. Indeed, let us consider, for RA, a rectangular array of diagonal length D as shown in Fig. 2-a.

The usual criterion for the far-field distance L is written as :

$$L = \frac{D^2}{\lambda} \qquad (1)$$

As shown in Fig. 2-b, that leads to an angle δ given by :

$$\tan \theta = \frac{\lambda}{2D} \qquad (2)$$

Which means that for the common case : $D >> \lambda$, the angle δ is small. From Fig. 2, if the lateral size of the Grill is of the same order as D, the angle δ' becomes small and the RA array must launch a very directive beam. Better is to envisage a lateral size of the Grill larger than D.

- Approximations will be detailed in the calculations. These calculations are managed in several steps : calculations of the reflection coefficient Γ at the end of a RA waveguide, far-field pattern of the TE_{10} mode, far-field pattern of the

RA array and radiated power within the angles of divergence, coupling of a plane wave to the TE_{10} mode in a Grill waveguide, and power transmission from the RA guides to the Grill guides.

II c - TE_{10} Reflection coefficient of a waveguide radiating into space

From [8], the equivalent circuit for the TE_{10} mode of a waveguide radiating into space is given in Fig. 3 with :

$$\frac{B'}{Y_0} = \frac{\sin t}{\cosh \pi x + \cos t} \qquad (3)$$

$$\frac{G'}{Y_0} = \frac{\sinh \pi x}{\cos \pi x + \cos t} \qquad (4)$$

where :

$$t = \frac{4\pi\zeta}{\lambda_g}$$

$$\zeta = \frac{\lambda_g}{2\pi} \times \left(x \ln \frac{2e}{\gamma x} - S_1(x) \right)$$

λ_g is the waveguide wavelength,
Y_O is the waveguide characteristic admittance,

$$S_1(x) = \sum_1^{\infty} \left((\sin \frac{x}{n})^{-1} - \frac{x}{n} \right)$$

and :

$$x = \frac{b}{\lambda_g}$$

b is the waveguide small size (Fig. 7)

$e = 2.718 \quad \gamma = 1.781$

from this the electric field reflection coefficient Γ can be determined by :

$$\Gamma^2 = \frac{(1 - G')^2 + B'^2}{(1+G')^2 + B'^2} \qquad (5)$$

The power reflection coefficient Γ^2 depends on the waveguide sizes a and b, and has been plotted on Fig. 4 for a varying from 7 to 13 cm and b from 3.4 to 8.4 cm by 0.2 step (Fig. 7). For a = 7.21 cm and b = 3.8 cm, its value is less than 8 % at a frequency of 3.7 GHz.

II d - Far-field radiation of the TE_{10} mode

Cartesian coordinates(x, y) are used in the aperture of RA array, and spherical coordinates (ρ, θ, ψ) are used to locate a point M in free-space, as shown in Figs. 5 and 6. From Ref. [3] and [4] the electric field E in the far-field is given by the following relations, where a constant factor is omitted :

$$E = \sqrt{E_\theta^2 + E_\psi^2}$$

$$E = \sqrt{\frac{\mu}{\varepsilon}} \frac{a^2 b}{\lambda^2 \rho} f(\theta,\psi) \qquad (6)$$

μ : magnetic permeability of medium,
ε : dielectric constant of medium,
λ : wavelength,
a,b, and the $\vec{E}$ field direction are defined at a waveguide aperture in Fig. 7.

The characteristic function is defined as the function of the radiated field depending of θ and ψ. In Eq. 6, it is f (θ,ψ) given by [5] :

$$f(\theta,\psi) = \sqrt{\sin^2\psi\left[1+\frac{\beta_{10}}{\beta}\cos\theta+\Gamma\left(1-\frac{\beta_{10}}{\beta}\cos\theta\right)\right]^2+\cos^2\psi\left[\cos\theta+\frac{\beta_{10}}{\beta}+\Gamma\left(\cos\theta-\frac{\beta_{10}}{\beta}\right)\right]^2}$$

$$\times \frac{\sin\left(\frac{\pi b}{\lambda}\sin\theta\sin\psi\right)}{\frac{\pi b}{\lambda}\sin\theta\sin\psi} \frac{\cos\left(\frac{\pi a}{\lambda}\sin\theta\cos\psi\right)}{\left(\frac{\pi}{2}\right)^2-\left(\frac{\pi a}{\lambda}\sin\theta\cos\psi\right)^2} \qquad (7)$$

where :

$\beta = \frac{2\pi}{\lambda}$ Free-space phase constant,

$\beta_{10} = \frac{2\pi}{\lambda}\sqrt{1 - \left(\frac{\lambda}{2a}\right)^2}$ TE_{10} mode phase constant,

Γ Reflection coefficient of the TE_{10} mode at the end of waveguide.

In the guide aperture, additional fields exist locally, excited by the discontinuity of the guide. Moreover, some currents are also distributed over the external surface of the waveguide. These additional fields and external currents are neglected in the calculation of $f(\theta, \psi)$ leading to Eq. 7.

The characteristic function $f_E(\theta, \psi)$ in the E plane is obtained for $\psi = \frac{\pi}{2}$, which gives, with a factor $\left(\frac{2}{\pi}\right)^2$ omitted :

$$f_E(\theta) = \left[1 + \frac{\beta_{10}}{\beta}\cos\theta + \Gamma\left(1 - \frac{\beta_{10}}{\beta}\cos\theta\right)\right]\frac{\sin\left(\frac{\pi b}{\lambda}\sin\theta\right)}{\frac{\pi b}{\lambda}\sin\theta} \qquad (8)$$

The characteristic function $f_H(\theta, \psi)$ in the H plane is obtained for $\psi = 0$:

$$f_H(\theta) = \left[\cos\theta + \frac{\beta_{10}}{\beta} + \Gamma\left(\cos\theta - \frac{\beta_{10}}{\beta}\right)\right]\frac{\cos\left(\frac{\pi a}{\lambda}\sin\theta\right)}{\left(\frac{\pi}{2}\right)^2 - \left(\frac{\pi a}{\lambda}\sin\theta\right)^2} \qquad (9)$$

In some situations, the knowledge of the power radiated by the TE_{10} mode within an angle $\theta = \theta_0$ is of special interest.

Using spherical coordinates, the radiated power is given by :

$$p = p_0 \int\int f^2(\theta,\psi)\sin\theta\, d\theta\, d\psi \qquad (10)$$

Where p_0 is a constant parameter.
The relation yielding the total radiated power p_R is :

$$p_R = 4\,p_0 \int_{\theta=0}^{\pi} \int_{\psi=0}^{\frac{\pi}{2}} f^2(\theta,\psi)\,\sin\theta\,d\theta\,d\psi \tag{11}$$

and for the power within an angle θ_0, it comes :

$$p_{\theta_0} = 4\,p_0 \int_{\theta=0}^{\theta_0} \int_{\psi=0}^{\frac{\pi}{2}} f^2(\theta,\psi)\,\sin\theta\,d\theta\,d\psi \tag{12}$$

or considering the normalized power p_{θ_0}/p_R :

$$\frac{p_{\theta_0}}{p_R} = \frac{\displaystyle\int_{\theta=0}^{\theta_0} \int_{\psi=0}^{\frac{\pi}{2}} f^2(\theta,\psi)\,\sin\theta\,d\theta\,d\psi}{\displaystyle\int_{\theta=0}^{\pi} \int_{\psi=0}^{\frac{\pi}{2}} f^2(\theta,\psi)\,\sin\theta\,d\theta\,d\psi} \tag{13}$$

II e - Far-field pattern of the RA array

Let us consider a rectangular plane array composed of infinitely small size RF sources units, regularly distributed in the x and y directions, as shown in Fig. 8. Each of these units works as an isotropic radiating source the amplitude and phase of all these sources being the same.

Using spherical coordinates as defined in Fig. 6, the characteristic function $F(\theta, \psi)$ or "Array Factor" is given by [3] [4] [6] :

$$F(\theta,\psi) = \frac{\sin(n_x \beta d_x \sin\psi \sin\theta)\,\sin(n_y \beta d_y \cos\psi \sin\theta)}{\sin(\beta d_x \sin\psi \sin\theta)\,\sin(\beta d_y \cos\psi \sin\theta)} \tag{14}$$

Where :

n_x number of units along the x direction,

n_y number of units along the y direction,
d_x and d_y are defined on Fig. 8.

In the E plane ($\psi = \frac{\pi}{2}$), the characteristic function becomes :

$$F_E(\theta,\psi) = n_y \frac{\sin(n_x \beta d_x \sin\theta)}{\sin(\beta d_x \sin\theta)} \qquad (15)$$

In the H plane ($\psi = 0$), the characteristic function is written as :

$$F_H(\theta,\psi) = n_x \frac{\sin(n_y \beta d_y \sin\theta)}{\sin(\beta d_y \sin\theta)} \qquad (16)$$

Then, one considers, for the units of array, identical rectangular waveguides where the TE_{10} mode propagates and has the same phase and amplitude in all guide apertures. From the principle of pattern multiplication, the characteristic function of the array Φ is given by [4] [6] :

$$\phi(\theta,\psi) = f(\theta,\psi)\, F(\theta,\psi) \qquad (17)$$

Where f and F are expressed by Eqs. 7 and 14.

In the E plane ($\psi = \frac{\pi}{2}$), the characteristic function Φ_E is written as :

$$\phi_E(\theta) = f_E(\theta)\, F_E(\theta) \qquad (18)$$

and it comes for the characteristic function Φ_H in the H plane ($\psi = 0$) :

$$\phi_H(\theta) = f_H(\theta)\, F_H(\theta) \qquad (19)$$

It has to be noted that in all the formulas related to radiations from the array, the coupling of the fields between the waveguides has been neglected.

A special feature of interest is the power radiated by this array within an angle $\theta = \theta_0$.

Using spherical coordinates, the radiated power is given by :

$$P = P_0 \int\int \phi^2(\theta,\psi)\, \sin\theta\, d\theta\, d\psi \tag{20}$$

Where P_0 is a constant parameter. The relation for the total radiated power P_R is :

$$P_R = 4\, P_0 \int_{\theta=0}^{\pi} \int_{\psi=0}^{\frac{\pi}{2}} \phi^2(\theta,\psi)\, \sin\theta\, d\theta\, d\psi \tag{21}$$

and for the power within an angle θ_0, it comes :

$$P_{\theta_0} = 4\, P_0 \int_{\theta=0}^{\theta_0} \int_{\psi=0}^{\frac{\pi}{2}} \phi^2(\theta,\psi)\, \sin\theta\, d\theta\, d\psi \tag{22}$$

or considering the normalized power p_{θ_0}/p_R :

$$\frac{P_{\theta_0}}{P_R} = \frac{\displaystyle\int_{\theta=0}^{\theta_0} \int_{\psi=0}^{\frac{\pi}{2}} \phi^2(\theta,\psi)\, \sin\theta\, d\theta\, d\psi}{\displaystyle\int_{\theta=0}^{\pi} \int_{\psi=0}^{\frac{\pi}{2}} \phi^2(\theta,\psi)\, \sin\theta\, d\theta\, d\psi} \tag{23}$$

II f - Coupling of an incident plane wave to the TE_{10} mode

Let us consider an incident plane wave impinging on a rectangular waveguide of the Grill. This wave is assumed to have a constant amplitude distribution. The geometrical parameters of the problem are defined in Fig. 9. It results from the phase and polarization properties of the TE_{10} mode, that the component of $\vec{E_i}$ which is taken into account in the calculation of the coupling of the incident wave to the TE_{10} mode at the guide aperture, must fulfil the following conditions :

1 - Polarization condition ; the component must be polarized along the x direction :

$$\begin{aligned} &E_{ix} \neq 0 \\ &E_{iy} = E_{iz} = 0 \end{aligned} \qquad (24)$$

2 - Phase condition : it has a constant phase in the guide aperture.

3 - Amplitude condition : its amplitude is derived from the flux of the Poynting vector through the aperture surface of the guide.

In the following calculations, the $\vec{E}_i$ component fulfilling this three conditions is determined, then the coupling coefficient of this $\vec{E}_i$ component to the TE_{10} mode is derived.

1 - Polarization condition. The waveguide axis and the TE_{10} polarization are the same in the RA and Grill waveguides. However, the polarization changes slightly in free-space, the wave front being spherical as shown in (Fig. 10) (Nevertheless, the incident wave front is assumed to be plane on the aperture of a waveguide of the Grill because this aperture is of small size).

The following relations hold for the wave Vector $\vec{k}$ and its components $\vec{k_x}$, $\vec{k_y}$, $\vec{k_z}$:

$$\left| \begin{aligned} k_x &= k \sin\theta \sin\psi \\ k_y &= k \sin\theta \cos\psi \\ k_z &= k \cos\theta \end{aligned} \right. \qquad (25)$$

and the amplitude E_{ix} is derived as (Fig. 10) :

$$E_{ix} = E_i \sqrt{1 - \left(\frac{k_x}{k}\right)^2} = E_i \sqrt{1 - (\sin\theta \sin\psi)^2} \qquad (26)$$

2 - Phase condition. It is assumed, because of the symmetry, that the phase of the TE_{10} mode excited in the aperture is that of the incident field $\vec{E}_i$ at the centre M of the aperture (Fig. 11).

The following relation comes :

$$E_M = E_{ix} \cos \omega t \tag{27}$$

$$E_N = E_{ix} \cos\left(\omega t - \vec{kr}\right) \tag{28}$$

Or considering E_{ixy}, the component of E_N with same phase as E_M (or the equiphase component) :

$$E_{ix\varphi} = E_{ix} \cos\left(- \vec{kr}\right) \tag{29}$$

Then, it comes :

$$\begin{aligned}\vec{kr} &= k_x\left(x-\frac{b'}{2}\right) + k_y\left(y-\frac{a'}{2}\right) \\ &= k \sin\theta\left[\sin\psi\left(x-\frac{b'}{2}\right) + \cos\psi\left(y-\frac{a'}{2}\right)\right]\end{aligned} \tag{30}$$

Finally, the equiphase component E_{ixy} is written as :

$$E_{ix\varphi} = E_i \sqrt{1 - (\sin\theta\sin\psi)^2}\, \cos\left\{k \sin\theta\left[\sin\psi\left(x-\frac{b'}{2}\right) + \cos\psi\left(y-\frac{a'}{2}\right)\right]\right\} \tag{31}$$

3 - Amplitude Condition. The power P_e entering the guide is given by :

$$P_e = \Pi\, a'b' \frac{k_z}{k} \tag{32}$$

Where π is the amplitude of the Poynting vector and is expressed by :

$$\Pi = \sqrt{\frac{\varepsilon_0}{\mu_0}} \frac{E_i^2}{2} \tag{33}$$

Then, P_e is written as :

$$P_e = \sqrt{\frac{\varepsilon_0}{\mu_0}} \frac{E_i^2}{2} a'b' \cos\theta \tag{34}$$

Which means that the amplitude E_e of the entering field into the guide is simply related to E_i by :

$$E_e = E_i \sqrt{\cos\theta} \tag{35}$$

Taking into account the conditions 1, 2 and 3, the field E_a in the guide aperture which is considered in the calculations of the coupling to the TE_{10} mode is given by :

$$E_a(x,y,\theta,\psi) = E_i \sqrt{\cos\theta}\ \sqrt{1-(\sin\theta\ \sin\psi)^2}\ \cos\left\{k\ \sin\theta\left[\sin\psi\left(x-\frac{b'}{2}\right)+\cos\psi\left(y-\frac{a'}{2}\right)\right]\right\} \tag{36}$$

The field E_a is assumed to be coupled to modes in the rectangular waveguides by the relation :

$$E_a = E\sin\frac{\pi y}{a'}e^{j\varphi} + \sum_{m=2}^{\infty}\sum_{n=1}^{\infty} E_{mn}\sin\frac{m\pi y}{a'}\cos\frac{n\pi x}{b'}e^{j\varphi_{mn}} \tag{37}$$

Where the phase φ_a of E_a is supposed to be null, E and φ are the amplitude and phase of the TE_{10} mode (m = 1, n = 0) and E_{mn} and φ_{mn} those of components of others TE_{mn} and TH_{mn} modes (these modes being evanescent or not).

The following integral relation is derived :

$$\int_{y=0}^{a'}\int_{x=0}^{b'} E_a\sin\frac{\pi y}{a'}\,dy\,dx = \int_{y=0}^{a'}\int_{x=0}^{b'} E\sin^2\frac{\pi y}{a'}e^{j\varphi}\,dy\,dx +$$

$$\int_{y=0}^{a'}\int_{x=0}^{b'}\sum_{m=2}^{\infty}\sum_{n=1}^{\infty} E_{mn}\sin\frac{\pi y}{a'}\sin\frac{m\pi y}{a'}\cos\frac{n\pi x}{b'}e^{j\varphi_{mn}}\,dy\,dx \tag{38}$$

Which leads to :

$$\varphi = 0 \tag{39}$$

and :

$$E = \frac{2}{a'b'} \int_{y=0}^{a'} \int_{x=0}^{b'} E_a \sin \frac{\pi y}{a'} \, dy \, dx \tag{40}$$

Starting from Eq. 35 it is possible to determine the power coupled from the incident to the TE_{10} mode.

The power P_g carried by the TE_{10} mode in a waveguide is given by [7] [8].

$$P_g = \sqrt{\frac{\varepsilon_0}{\mu_0}} \sqrt{1 - \left(\frac{\lambda}{2a'}\right)^2} \frac{a'b'}{4} E^2 \tag{41}$$

$$\text{or :} \quad P_g = \langle I_g \rangle \, a' \, b' \tag{42}$$

Where $\langle I_g \rangle$ is defined as the mean intensity of the TE_{10} mode in the waveguide.

In the following, we will consider a coupling coefficient $G(\theta, \psi)$ defined by :

$$G(\theta,\psi) = \frac{P_g}{P_i} = \frac{\langle I_g \rangle}{I_i} \tag{43}$$

Where P_i is the power of a beam crossing an area $S = a' \, b'$ with normal incidence, and I_i the corresponding intensity. They are given by :

$$P_i = \sqrt{\frac{\varepsilon_0}{\mu_0}} E_i^2 \, a'b' = I_i \, a'b' \tag{44}$$

and from Eqs. 36, 40, 41, 42, and 44, $G(\theta, \psi)$ is expressed by :

$$G(\theta,\psi) = \frac{P_g}{P_i} = \frac{2}{a'^2 b'^2} \sqrt{1 - \left(\frac{\lambda}{2a'}\right)^2} \cos\theta \left[1 - (\sin\theta \sin\psi)^2\right] \times \left[\int_{y=0}^{a'} \int_{x=0}^{b'} \cos\left\{k \sin\theta \left[\left(x - \frac{b'}{2}\right)\sin\psi + \left(y - \frac{a'}{2}\right)\cos\psi\right]\right\} \sin\frac{\pi y}{a'} \, dy \, dx\right]^2 \tag{45}$$

The coupling coefficient $G(\theta, \psi)$ is easily derived in the case of normal incidence. By making $\theta = 0$ in Eq. 45, it comes :

$$G(0,\psi) = \frac{8}{\pi^2}\sqrt{1-\left(\frac{\lambda}{2a'}\right)^2} = 0.811\sqrt{1-\left(\frac{\lambda}{2a'}\right)^2} \qquad (46)$$

The coupling coefficient is always lower than 0.811.

II g - Power transmission from the RA waveguides to the Grill waveguides

The beam power P_e entering the waveguides of the Grill is given by the flux of the Poynting vector through the Grill surface Σ_G or the spherical surface Σ_S as shown in Fig. 12.

P_E is expressed by :

$$P_E = P_0 \int\int_{\Sigma_s} I(\theta,\psi)\sin\theta\, d\theta\, d\psi \qquad (47)$$

or :

$$P_E = P_0 \int\int_{\Sigma_G} I(\theta,\psi)\cos\theta\, dx'\, dy' \qquad (48)$$

The factor cos θ vanishes in the integral over Σ_S as the Poynting vector is normal to the surface. In the following, the constant parameter P_0 will not be expressed.

From Eq. 43 it comes :

$$I_g(\theta,\psi) = G(\theta,\psi)\, I_i(\theta,\psi) = g(\theta,\psi)\cos\theta\, I_i(\theta,\psi) \qquad (49)$$

With :

$$g(\theta,\psi) = \frac{G(\theta,\psi)}{\cos\theta} \qquad (50)$$

Calculating the power P_G of the TE_{10} mode in the Grill, it is more convenient to use the integration over Σ_S (Eq. 47) than over Σ_G (Eq. 48). That yields :

$$P_G = \int\int_{\Sigma_s} I_i(\theta,\psi)\, g(\theta,\psi) \sin\theta \, d\theta \, d\psi \tag{51}$$

or from Eqs. 20 and 51 :

$$P_G = \int\int_{\Sigma_s} \phi^2(\theta,\psi)\, g(\theta,\psi) \sin\theta \, d\theta \, d\psi \tag{52}$$

Where a constant parameter is omitted, and $\Phi(\theta, \psi)$ is given by Eq. 17.

From Fig. 12, the limits of integration over Σ_S can be easily determined, leading to the following relation for P_G :

$$P_G = 4\left[\int_{\psi=0}^{\sin^{-1}\frac{B}{A}} d\psi \int_{\theta=0}^{\theta_M=\sin^{-1}\left(\frac{1}{\cos\psi}\right)} \phi^2(\theta,\psi)\, g(\theta,\psi) \sin\theta \, d\theta + \int_{\psi=\sin^{-1}\frac{B}{A}}^{\frac{\pi}{2}} d\psi \int_{\theta=0}^{\theta_M=\sin^{-1}\left(\frac{1}{\sin\psi}\right)} \phi^2(\theta,\psi)\, g(\theta,\psi) \sin\theta \, d\theta\right] \tag{53}$$

When deriving this Eq. 53, two main approximations have been assumed :

- The thickness of the guide walls of the Grill are neglected, which gives no reflection of the incident beam.

- The diffraction by the guide edges and the field coupling between the guides of the grill are not taken into account.

Let us consider the total power P_T in the guides of RA. It is related to the reflection coefficient of the amplitude Γ, at the end of the guide, and to the total beam power P_R radiated from RA by the relation :

$$P_T = \frac{P_R}{1 - \Gamma^2} \tag{54}$$

Which can be written as :

$$P_T = \frac{4}{1 - \Gamma^2} \int_{\theta=0}^{\pi} \int_{\psi=0}^{\frac{\pi}{2}} \phi^2(\theta,\psi) \sin\theta \, d\theta \, d\psi \qquad (55)$$

Where $\Phi(\theta, \psi)$ is given by Eq. 17.

Finally the power transmission T in the TE_{10} mode between the guides of RA and the guides of the Grill is given by :

$$T = \frac{P_G}{P_T} \qquad (56)$$

III - APPLICATION

Numerical applications of formulas derived in Section II, are achieved for two frequencies : f = 3.7 GHz (case of JET and Tore-Supra) and f = 8 GHz (maximum possible frequency for ITER). The size of the rectangular waveguides is defined by (Fig. 7).

a = a' = 72.1 mm
b = b' = 38 mm

Where (a, b) corresponds to RA guides and (a', b') to Grill guides.

These values of a and b come from a preliminary design of a quasi-optical antenna for JET. The same values are arbitrarily considered for a' and b'. In fact, the following applications are only examples and cannot be looked as specific values for a given Tokamak.

Considering the RA array, the calculations are made with the following parameters [Fig. 5 and Eq. 14]

$n_x = 8$ $\quad 2 d_x = 45$ mm
$n_y = 6$ $\quad 2 d_y = 80$ mm

For the power transmission from RA to the Grill, four different values of A and B are taken into account [Figs. 2 and 12].

1 -	2 A	=	938 mm	2 B	=	456 mm
2 -	2 A	=	1876 mm	2 B	=	912 mm
3 -	2 A	=	3752 mm	2 B	=	1824 mm

The values of the case 1 have been chosen because they fitted well the Grill size of the JET. The values 2 and 3 are multiple of values 1, in order to scale the sensitivity of the transmission with the Grill size.

III a - TE_{10} mode

The far-field pattern $f_E(\theta)$ and $f_H(\theta)$ of the TE_{10} mode in the E and H planes are shown in Figs. 13 - 16. The normalized radiated power P_{θ_0}/P_R , (Eq. 13), within an angle $\theta = \theta_0$ is shown in Fig. 17. The results emphasize the weakness of the directivity of the TE_{10} mode, even for $f = 8$ GHz and oversized guide.

III b - RA array

The far-field pattern in the E and H planes are shown in Figs. 18, 21. The normalized power within an angle $\theta = \theta_0$ is shown in Fig. 22. By comparison to a single waveguide radiation, the directivity is clearly improved. Nevertheless, an important level of power is always lost in the secondary lobs, which limits the interest for this type of array.

III c - Coupling

The coupling coefficient $G(\theta)$ is displayed in Figs. 23 and 24 for different values of ψ. In Figs. 25 and 26 a space representation of $G(\theta, \psi)$ is shown. The main result is that $G(\theta)$ is very sensitive to the angle θ and decreases quickly for θ larger than 10-20 d°, which means that the incident beam must be very directive.

III d - Transmission

The power transmission T, defined by Eq. 56 is displayed versus the distance L in Figs. 27 and 28. The calculation is valid only in the far-field region, i.e. for

L > 4.500 mm (full line). In the near-field region (L < 4.500 mm) the calculation is no more exact but gives an indication of the variation of T. As the main result, the transmission T is always small in the far-field, even for large size Grill, while some improvements are expected in the near-field region.

IV - IMPROVEMENT OF WAVEGUIDE ARRAYS DIRECTIVITY BY THE DOLPH METHOD

For an array of 2n sources which are distant from a distance 2d the radiated electric field can be written as (Fig. 29).

$$E = A_1 e^{js/2} + A_2 e^{j3s/2} + ... + A_n e^{j(2n-1)s/2} + A_1 e^{-js/2} + A_2 e^{-j3s/2} + ... + A_n e^{-j(2n-1)s/2} \quad (57)$$

if the sources which are symmetric are fed with the same power and with :

$$s = 2\pi\xi + 2\beta d \sin\theta \cos\psi \quad (58)$$

where $\beta = 2\pi/\lambda$, λ is the wavelength and θ and ψ are defined in Fig. 30.
$2\pi\zeta$ is the phase shift supposed constant between each source.
E can be also written as :

$$E = 2[A_1 \cos s/2 + A_2 \cos 3s/2 + ... + A_n \cos (2n-1)s/2] \quad (59)$$

If we note T_{2n-1} the tchebychev polynomial of order 2n-1, E can also be defined as follow :

$$E = 2[A_1 T_1(\cos s/2) + A_2 T_3(\cos s/2) + ... + A_n T_{2n-1}(\cos s/2)] \quad (60)$$

The Dolph method allows to choose the different amplitude A_n to fix the ratio R of the main lobe to the one of the 1st secondary lobe. For this one has to compute the value x_0 which is given by :

$$x_0 = \frac{1}{2}\left[\left(R+\sqrt{R^2-1}\right)^{1/(2n-1)} + \left(R-\sqrt{R^2-1}\right)^{1/(2n-1)}\right] \quad (61)$$

The polynomial $T_{2n-1}(x)$ can be defined as :

$T_{2n-1}(x) = \overline{T_{2n-1}}\ \overline{X'}$

with

$\overline{T_{2n-1}} = (a_1 , a_2 , ... , a_{2n-1})$

and

$\overline{X} = (x , x^2 , ... , x^{2n-1})$

$\overline{X'}$ is the column vector transposed of $\overline{X}$.
The coefficients $A_1, A_2,.....,A_{2n-1}$ are then computed using the following relation :

$\overline{A'} = \overline{\overline{M^{-1}}}\ \overline{T'_{2n-1}}$

with :

$\overline{\overline{M}}$ the squared matrix build with :

$\overline{\overline{M}} = (\overline{T'_1}(1/x_0) , \overline{T'_3}(1/x_0) , ... , \overline{T'_{2n-1}}(1/x_0))$

In our case for which we have 8 sources along the x direction and 6 ones along the y direction, the Dolph method can be applied separately. First the coefficients A1, A2, A3, A4 and B1, B2, B3 have been calculated depending on the ratio R. On Fig. 31 the ratio of the different coefficients on A1 (B1) are plotted versus the ratio R.

For example for 8 sources and with a ratio R = 50 the coefficients Ai are :

A1 = 1
A2 = 0.78
A3 = 0.47
A4 = 0.20.

On Fig. 32 the ratio η of the power in a given cone of half angle θ to the total radiated power is plotted versus the value of θ for 2 case :

- the first one for an equally fed network.
- the second using the Dolph method where a value of R = 100 has been taken.

It may be observed that there is a large increase up to an angle of 15 degrees where η reaches 0.57 in the first case and 0.7 for the second one.

In order to improve the efficiency η, the distance dy separating the source in the vertical direction has been changed from 40 mm to 35 mm. On Fig. 32 it can be seen that η reaches 0.8 for the equaly fed case and 0.93 with the Dolph method where R = 100 has been taken.

On Figs. 33 and 34 the electric field radiation pattern had been drawn depending on θ and ψ for dy = 35 mm. The secondary lobe amplitude decrease can be shown very well when the Dolph method is applied.

V - OTHER CONCEPTS USING RECTANGULAR WAVEGUIDES BUT ADDING FOCUSSING DEVICES

As the calculations result in low power transmission between the RA and the Grill in the basic scheme, other concepts are qualitatively described in the present section, using focussing devices in order to improve the directivity and the transmission of the system.

V a - The free-space between RA and the Grill is surrounded by an ellipsoid mirror with a circular symmetry as shown in Fig. 35. The focus F_1 and F_2 of the mirror are located on the axis of the system and in the aperture of RA and the Grill.

- Advantages : Most of the power radiated from RA impinges on the Grill. The device is rather compact.

- Disadvantages : Some rays have a large angle of incidence on the Grill, which result in a low coupling to the TE_{10} mode in the Grill.

V b - A large ellipsoid mirror reflects the beam from RA to the Grill, the focus F_1 and F_2 being located in the middle of the Grilland RA apertures, as shown in Fig. 36. The grill and RA apertures have the same size.

- Advantages : Most of the power radiated from RA impinges on the Grill. For beams radiated from RA with a good directivity, the angle of incidence on the Grill keeps small.

- Disadvantages : The mirror and all the device must be large in order to achieve a good transmission.

V c - In the present concept, RA does not work as an array : the beams radiated from each waveguide of RA are independently considered (Fig. 37). A focussing mirror is associated to each waveguide (ended with/without a horn) in order to achieve the same beam section recovering all the Grill aperture. Moreover, the distances are adjusted so that the beams have the same phase on the Grill.

- Advantages : By comparison to the array systems the launching aperture of each guide is larger, the mirror M smaller, and the far-field region nearer.

- Disadvantages : For a large number of emitting waveguides, the RA size becomes large. In fact, this concept may replace the array concept for a small number of RA waveguides.

V d -The theoretical designs of the preceding concepts show that a good power transmission would be difficult to achieve, even with focussing devices, large size systems... The use of metallic lenses instead of mirrors would not change drastically the situation. An improvement would be gained by putting the Grill in the near-field of the emitting array, but that seems not to be sufficient, mainly because of the rather bad coupling of the incident wave to the TE_{10} mode in the Grill.

VI - CONCEPTS BASED ON GAUSSIAN BEAMS AND OPTICAL ROD ARRAYS

In order to improve the beam directivity and the coupling to the Grill, Gaussian beams are considered as well as a system of rod arrays for the Grill (Figs. 38 and 39).

The main advantages of Gaussian beams are :

- Low divergence is achieved if the beam waist diameter is large enough.
- The field has the same linear polarization in all the beam.
- The beam is circularly symmetric.
- The laws of propagation and focussing are well-known.

The Gaussian beam is launched from a circular oversized waveguide where a HE_{11} mode propagates. Thus, a mode conversion is needed after the sources in order to obtain the HE_{11} mode in the RA.

VII - WAVEGUIDES FOR HE_{11} MODE

In this section, some waveguide structures and size, well fitted for the HE_{11} mode in the LH frequency range (3.7 - 8 GHz) are determined. Three types of circular waveguides are used for propagation of the HE_{11} mode :

- The smooth waveguide with dielectric or low-conducting wall material. This type of guide is largely used in laser systems [9] [10] [11].
- The dielectric lined waveguide, also experimented in laser and infrared transmission [11] [12].
- The corrugated metallic waveguide, scheduled for some Electron Cyclotron Experiences at mm wavelength [11] [13] [14].

A power attenuation constant α of the HE_{11} mode in a guide is defined by :

$$\alpha = -\frac{1}{P}\frac{dP}{dz} \tag{62}$$

where P is the mode power.

- In smooth oversized waveguides, with dielectric or low-conducting wall material, the attenuation is given by [10] [11].

$$\alpha = \frac{8\,u_{11}^2}{k^2 D^3}\frac{v_1^2 + 2}{v_1}\cos\phi_1 \tag{63}$$

where :

$$v_1 = \left[(\varepsilon_r - 1)^2 + \left(\frac{\sigma^2}{\varepsilon_0\omega}\right)^2\right]^{\frac{1}{4}} \tag{64}$$

$$\phi_1 = \frac{1}{2}\tan^{-1}\left[\frac{\sigma}{\varepsilon_0\omega(1 - \varepsilon_r)}\right] \tag{65}$$

ε_r and σ are respectively the relative dielectric constant and the conductivity of the material, ε_0 the free-space dielectric constant, u_{11} the first root of the first kind Bessel function $J_0(x)$, ($u_{11} = 2{,}405$), k the free-space propagation constant ($k = \frac{2\pi}{\lambda}$) and D, the guide diameter.

In order to achieve lo *w*-loss transmission, the optimal theoretical material characteristics are derived as [10] [11] :

$$\left| \begin{array}{rcl} \varepsilon_r & = & 1 \\ \sigma & = & 2\varepsilon_0\omega \end{array} \right. \qquad (66)$$

and from Eqs. 63 to 66, it comes :

$$\alpha = 2.344 \frac{\lambda^2}{D^3} \text{ m}^{-1} \qquad (67)$$

where λ and D are expressed in mm.

Eq. 67 is plotted versus D for the frequencies $f = 3.7$ GHz and $f = 8$ GHz in Fig. 40.

- Let us consider a dielectric lined waveguide as shown in Fig. 41. The attenuation α has been derived by an optical model in Ref.[11], for oversized waveguides. That yields :

$$\alpha = \frac{8\sqrt{2}u_{11}^2}{k^2 D^3 v'} \left[\frac{v^4}{(v^2 - 1)(1 - \cos\psi)} + \frac{1}{1 + \cos\psi} \right] \qquad (68)$$

Where v is the refractive index of the dielectric, v' is the modulus of the complex refractive index of the metal $\overline{v'}$, related to the conductivity σ by :

$$\overline{v'} = \sqrt{\varepsilon_r - j\frac{\sigma}{\varepsilon_0\omega}} \qquad (69)$$

and the angle ψ is given by :

$$\psi = 2kd\sqrt{v^2 - 1} \qquad (70)$$

In Eq. 68 the refractive index υ is assumed to be real (losses in the dielectric are neglected). It is shown in Ref. 11, that the minimum theoretical value of α is achieved for :

$$\nu = \sqrt{2}$$
$$2kd = \pm \cos^{-1}\left(\frac{1}{3}\right) \pm (2p+1)\pi \qquad (71)$$

and assuming the wall made with copper, the conductivity σ has the following typical value in the microwave range :

$$\sigma = 4\ 10^{-7}\ \text{mhos} \qquad (72)$$

From Eqs. 68, 71 and 72, the minimum value α is derived as :

$$\sigma = 4.794\ \frac{\lambda^2}{D^3\sqrt{\lambda}}\ m^{-1} \qquad (73)$$

where D and λ are expressed in mm , Eq. 73 is plotted versus D for the frequencies f = 3.7 GHz and f = 8 GHz in Fig. 42.

- In corrugated oversized waveguides, the attenuation is given by : [13]

$$\alpha = \frac{8\ u_{11}^2}{D^3 k^2} \sqrt{\sqrt{\frac{\varepsilon_0}{\mu_0}}\ \frac{\pi}{\sigma\lambda}}\ (\alpha_1 + \alpha_2) \qquad (74)$$

where :

$$\alpha_1 = \frac{1 - \frac{t}{h} + \frac{\lambda}{4h}}{\left(1 - \frac{t}{h}\right)^2}$$
$$\alpha_2 \approx 1$$
$$d = \frac{\lambda}{4} \qquad (75)$$

The parameters d, t and h are defined in Fig. 43. Let us consider a corrugated waveguide defined by the following parameters :

$$\sigma = 4\ 10^{-7} \text{ mhos}$$
$$t = \frac{\lambda}{4}$$
$$h = \frac{\lambda}{2} \qquad (76)$$

From Eqs. 74 and 76 the attenuation is written as :

$$\alpha = 2.682 \frac{\lambda^2}{D^3\sqrt{\lambda}} \text{ m}^{-1} \qquad (77)$$

where D and λ are expressed in mm.

This Eq. 77 is plotted versus D for the frequencies f = 3.7 GHz and f = 8 GHz in Fig. 44.

From Figs. 40, 42 and 44 it is shown that the HE_{11} mode can propagate in oversized dielectric lined or corrugated waveguides with very small losses, even for long waveguide. The choice between the dielectric lined waveguide and the corrugated waveguide depends mainly on some problems as : manufacturing, breakdowns, vacuum, cost...

VIII - GAUSSIAN BEAM RADIATION FROM HE_{11} MODE

The HE_{11} radiated field can be well approximated by a Gaussian distribution in the far-field and even in some part of the guide aperture near-field [16]. The main advantages of the Gaussian beams, compared to other mode radiations are :

- A low divergence may be achieved (the beam waist diameter must be large enough for this purpose).
- No secondary patterns exist.
- The Electric field has the same linear polarization in all the beam.
- The beam is circularly symmetric.
- The laws of propagation and focussing are well known.

The Gaussian beam intensity is given by :

$$I(\rho,z) = I(0,z)\, e^{\left[-\frac{\rho^2}{r^2(z)}\right]} \qquad (78)$$

Where z is the abscissa along the propagation axis, ρ is the radial coordinate, and r defined as the beam radius is the value of ρ for which the intensity is 1/e times the on axis value (Figs. 45 and 46). In some papers, the radius w of the field amplitude is considered and is defined as the value of ρ for which the amplitude is 1/e times the on axis value. Hence, the following relation holds :

$$w = z\sqrt{2} \tag{79}$$

The radius r depends on the abscissa z, according to the relation :

$$r^2(z) = r_0^2 + \frac{z^2}{k^2 r_0^2} \tag{80}$$

The beam contracts to a minimum radius r_0 at the beam waist ($z = 0$). Far from the waist, within the condition $z >> kr_0^2$, Eq. 80 becomes :

$$r(z) = \frac{z}{kr_0} \tag{81}$$

and, an angle of divergence of the Gaussian beam is defined as :

$$\theta_0 = \frac{r}{z} = \frac{1}{kr_0} \tag{82}$$

This definition is valid only for the usual case of the paraxial approximation : $\theta_0 << 1$.
The beam power P_a through a circular section of radius $\rho = a$ is given by :

$$\begin{aligned} P_a &= \int_{\rho=0}^{a} \int_{\psi=0}^{2\pi} I(0,z)\, e^{\left(-\frac{\rho^2}{r^2}\right)} \rho \, d\rho \, d\psi \\ &= \pi\, I(0,z)\, r^2(z) \left[1 - e^{\left(-\frac{a^2}{r^2}\right)}\right] \\ &= P_T \left[1 - e^{\left(-\frac{a^2}{r^2}\right)}\right] \end{aligned} \tag{83}$$

Where P_T is the total beam power.

For $z >> kr_0^2$, Eq. 83 can be written as :

$$\frac{P_\theta}{P_T} = 1 - e^{\left(-\frac{\theta^2}{\theta_0^2}\right)} \tag{84}$$

Where P_θ is the beam power within the angle θ. Eq. 84 is plotted in Fig. 47, showing that for $\theta > 2\theta_0$, most of the power locates inside the angle θ. The Gaussian beam radiated by the HE_{11} mode has a fictitious waist located at the guide aperture, and its diameter d_0 is simply related to the diameter D of the guide by the relation [16] :

$$d_0 = 0.42\ D \tag{85}$$

Let us consider the value $\theta = 2{,}2\ \theta_0$ for which :

$\frac{P_\theta}{P_T} = 0.99$ and $\theta = 1.8\ \theta_0$ for which $\frac{P_\theta}{P_T} = 0.96$

These values of θ are plotted versus the waist diameter d_0 and the guide diameter D, for the frequencies $f = 3.7$ GHz and $f = 8$ GHz in Fig. 48. This Figure shows that small angle of divergence can be achieved for large guide diameters. In any case, for small guide diameters, focussing systems can be added resulting in low divergent Gaussian beam, before impinging the Grill.

IX - QUASI-OPTICAL GRILL

A quasi-optical Grill has been proposed by Petelin and Suvorov [1] and by Kovalyov et al. [2]. This system is composed of a metallic rod array. In order to improve the transmission, theoretically up to 100 %, a two layers Grill structure is considered. This system looks to be attractive by comparison to the classical waveguide structure. In order to achieve a good transmission, a low diverging incident beam is required, and accordingly an adequate solution is to use a suitable Gaussian beam for this incident beam.

X - CONCLUSION

Two types of LHW launchers, based on quasi-optical propagation between Radiating Antennas and the Grill have been considered.

The first type, using rectangular waveguide arrays for RA and the Grill, leads to low power transmission values . In the best case 70 % of the total incident power is radiated in a beam within a divergence angle of 20 degrees .An improvement of the emission pattern by feeding the waveguides with different amplitude according to the Dolph Tchebycheff method gives only a small increase. The best improvement is obtained when

the periodicity of the waveguide is changed .In that case more than 90 % of the total power is radiated within an angle of emission of 10 degrees. The coupling of the incident wave to the TE10 mode in the grill waveguides is shown to be always lower than 81 % . The fact that the grill is in the far field from the source explains the low transmission factor . The transmission can be improved by putting the grill in the near field region and by using oversized waveguide in the grill to increase the coupling coefficient, but the computation of such a structure is quite a difficult task .

In the second type, Gaussian beams are launched by RA in order to have a smaller angle of divergence and therefore to improve the emission . The Gaussian beam would be radiated from circular corrugated waveguides propagating the HE11 mode . More than 95 % of the incident power can be radiated in an angle of emission of less than 5 degrees if the waveguides are highly oversized. The Grill is composed of rod arrays which could be easily water cooled and therefore which could withstand the thermal flux due to the plasma better than the grill with waveguides . This concept looks to be attractive as a good transmission and directivity are expected. But for the grill one has to use 2 rows of rod array in order to decrease the standing wave ratio due to the sizes of the rods used to excite a good N// spectra leading by this way to a structure highly resonant . However, more thorough theoretical and experimental studies are needed, in order to make this concept more precise and to compare it to LHW launchers based strictly on waveguide concepts.

REFERENCES

[1] Quasi-optical Grill for excitation of lower hybrid waves in a toroidal Plasma.
M.I Petelin and E.V. Suvorov.
Sov. Tech. Phys. Lett. 15 (11), Nov. 1989.

[2] Quasi-optical Grill for excitation of Lower-Hybrid waves in a Plasma.
N.F. Kovalyov, M.I. Petelin, E.V. Suvorov,
S.E. Fil' chenkov.
Int. Workshop "Strong microwaves in Plasmas".
Suzdal, URSS, Sept. 18-23, 1990.

[3] Théorie et technique des Antennes.
L. Eyraud, G. Grange, H. Ohanessian.
Vuibert.

[4] Les Antennes.
L. Thourel.
Dunod.

[5] Microwave Antenna theory and design.
S. Silver.
Dover Publications.

[6] Antennas and radio-wave propagation.
R.E. Collin.
Mc Graw-Hill Book Company.

[7] Les Ondes Centimétriques.
G. Raoult.
Masson.

[8] Waveguide Handbook.
N. Marcuvitz.
Mc Graw-Hill Book Compagny.

[9] The Waveguide Laser : A Review.
J.J. Degnan.
Appl. Phys. 11 (1) 1976.

[10] Mode Propagation Constants in Hollow Oversized Circular Waveguides with Low-Conductivity Wall Material.
J.P. Crenn, P. Belland.
Int. J. Inf. Mm Waves 7 (10) Oct. 1986.

[11] Atténuation des modes dans les guides d'ondes circulaires surdimensionnés pour ondes millimétriques et submillimétriques. Comparaison des modes principaux dans différents types de guides.
J.P. Crenn.
Rap. EUR - CEA - FC 1311 (1986).

[12] Fabrication of germanium-coated nickel hollow waveguides for infrared transmission.
M. Miyagi, A. Hongo, Y. Aizawa, S. Kawakami.
Appl., Phys., Lett. 43 (5) Sept. 1983.

[13] Attenuation and Radiation Characteristics of the HE_{11} mode.
C. Dragone.
IEEE Trans. Microwave Th. Tech. 28 (7) July 1980.

[14] Propagation and Mode Coupling in Corrugated and smooth-Wall Circular Waveguides.
J. Doane.
Inf. and Mm Waves 13 (5), Academic Press (1985).

[15] Study on EC W Transmission lines for NET/ITER.
W. Henle, A. Jacobs, W. Kasparek, H. Kumric, G.A. Müller, P.G. Schüller, M. Thumm.
NET Report EUR-FU/80/90-99 (Oct. 1990).

[16] Radiation patterns of the HE_{11} mode and Gaussian approximations.
L. Rebuffi, J.P. Crenn.
Int. J. Inf. Mm Waves 10 (3) March 1989.

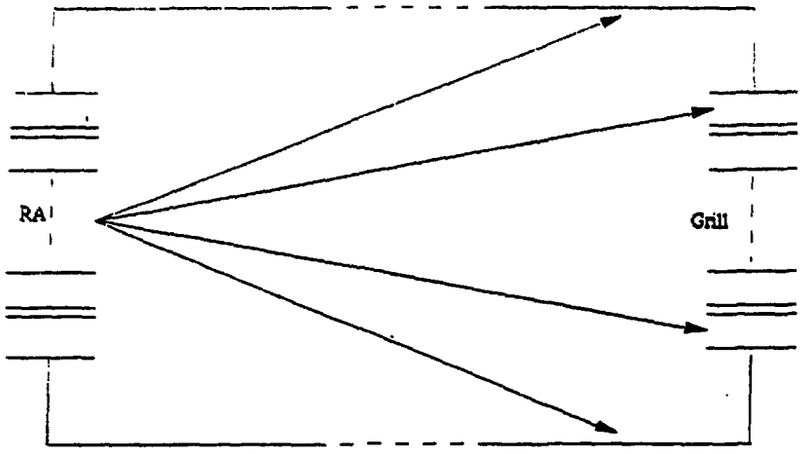

Fig 1

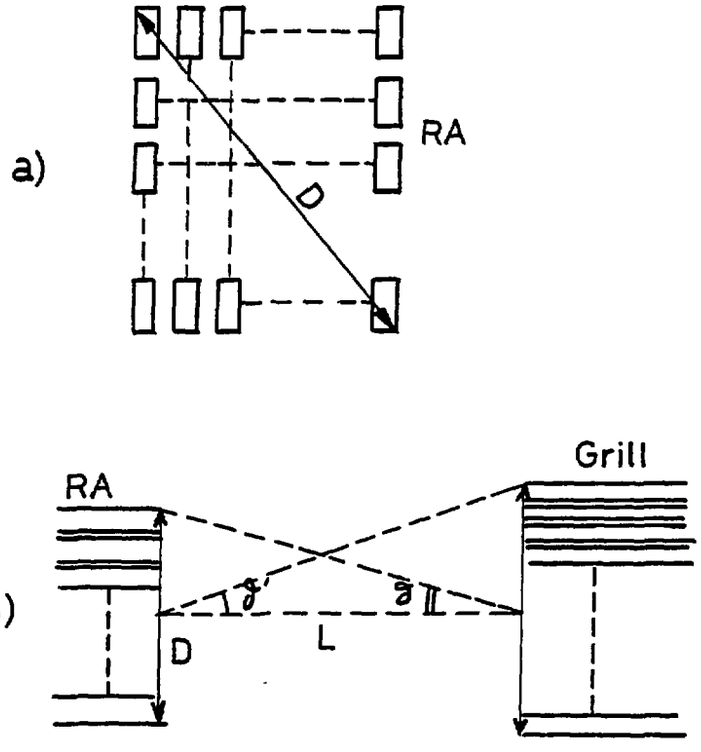

-Fig 2-

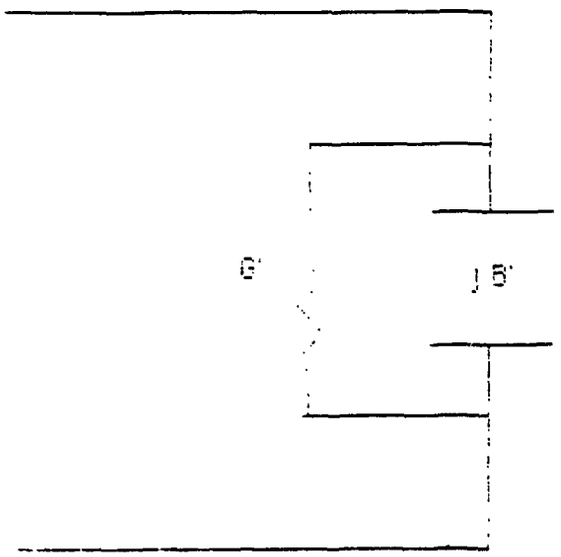

figure 3

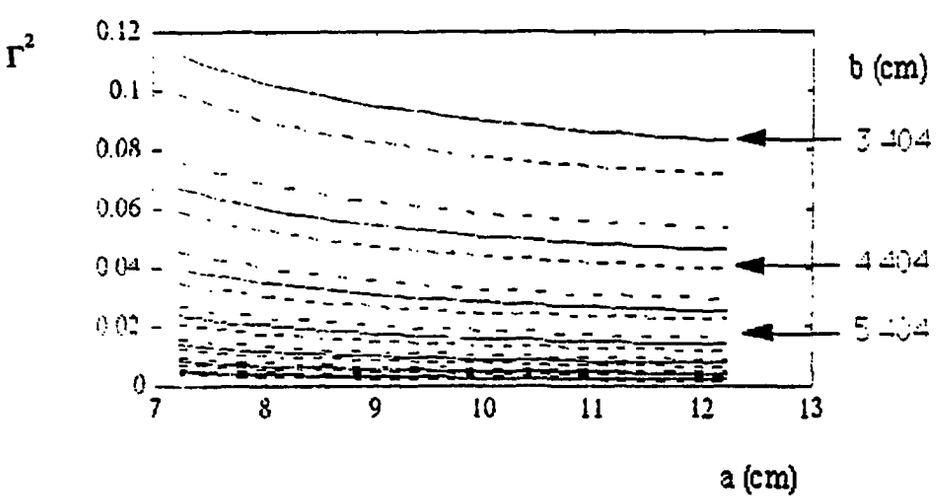

Fig (4)

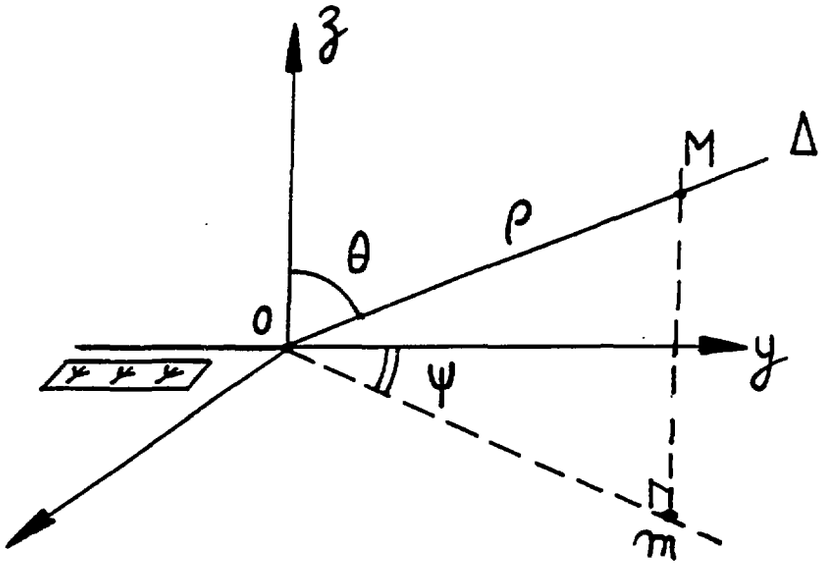

- Fig 6 -

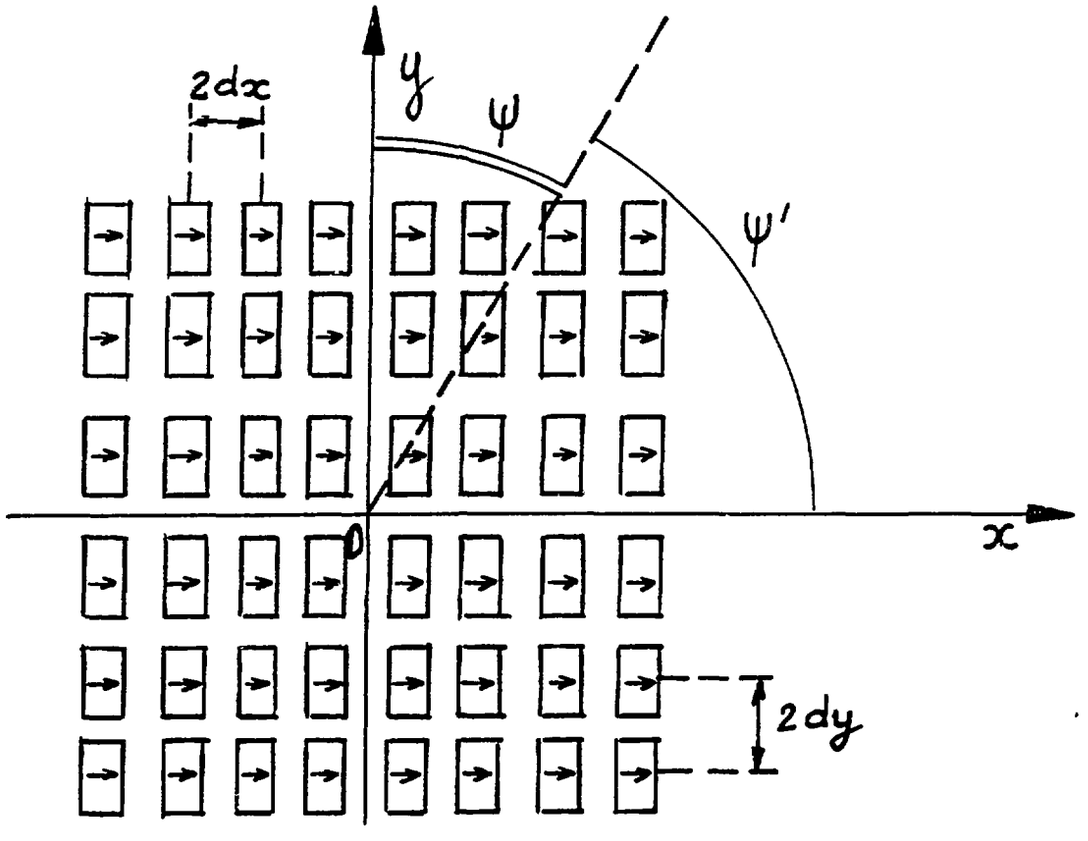

- Fig 5 -

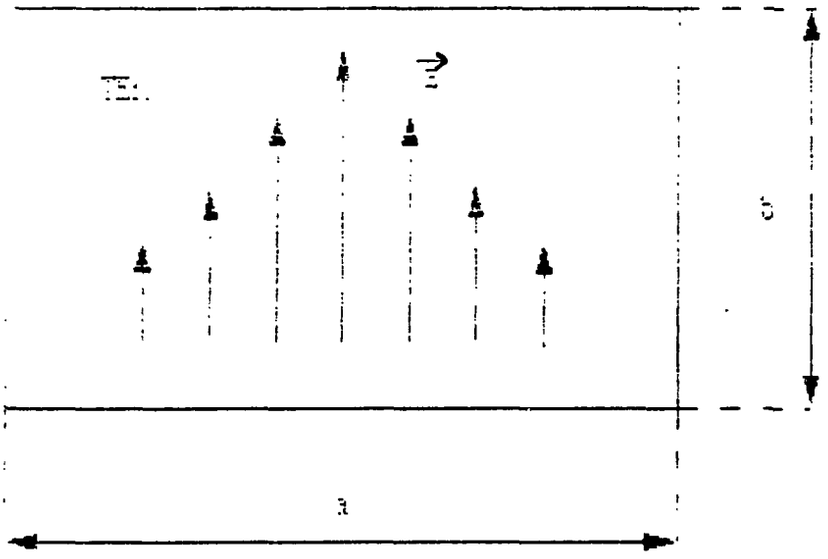

Fig 7

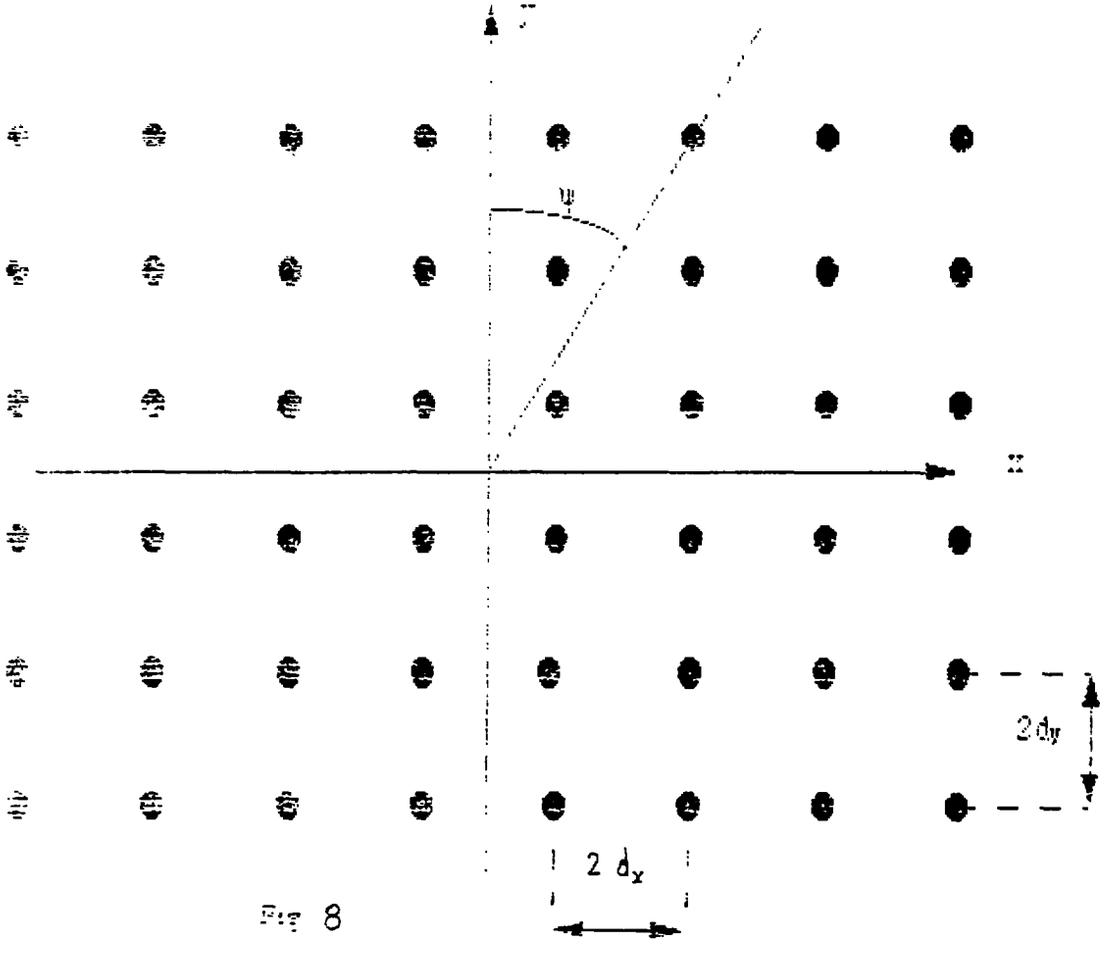

Fig 8

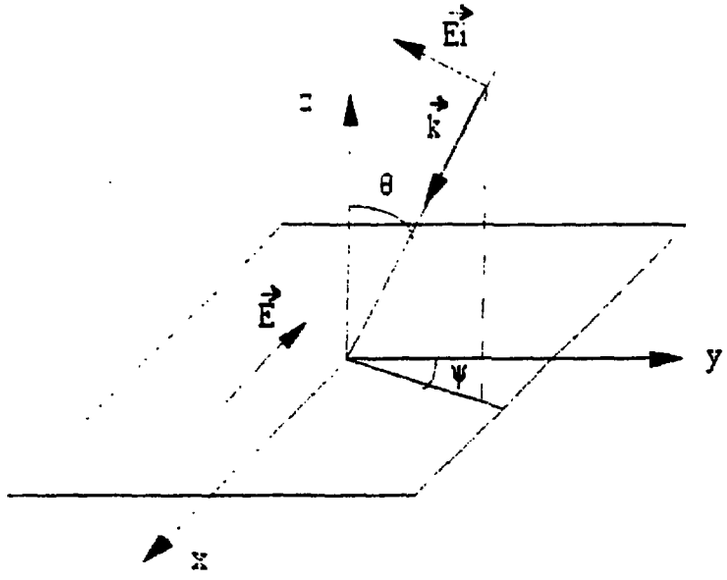

Fig 9

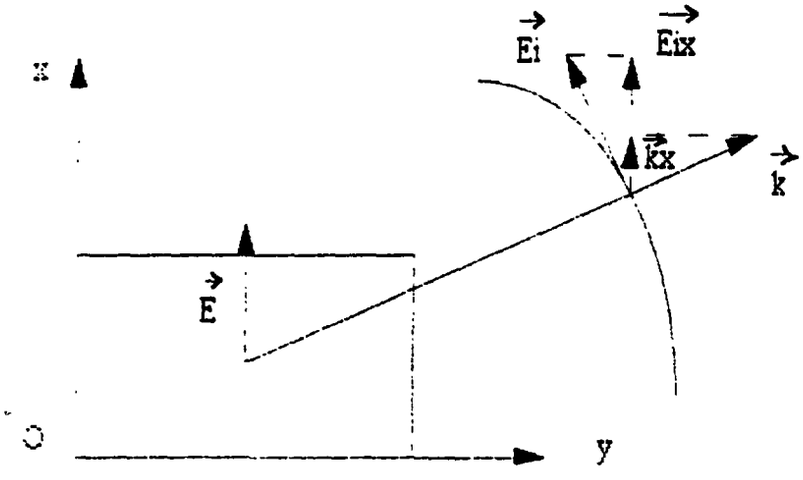

Fig 10

x

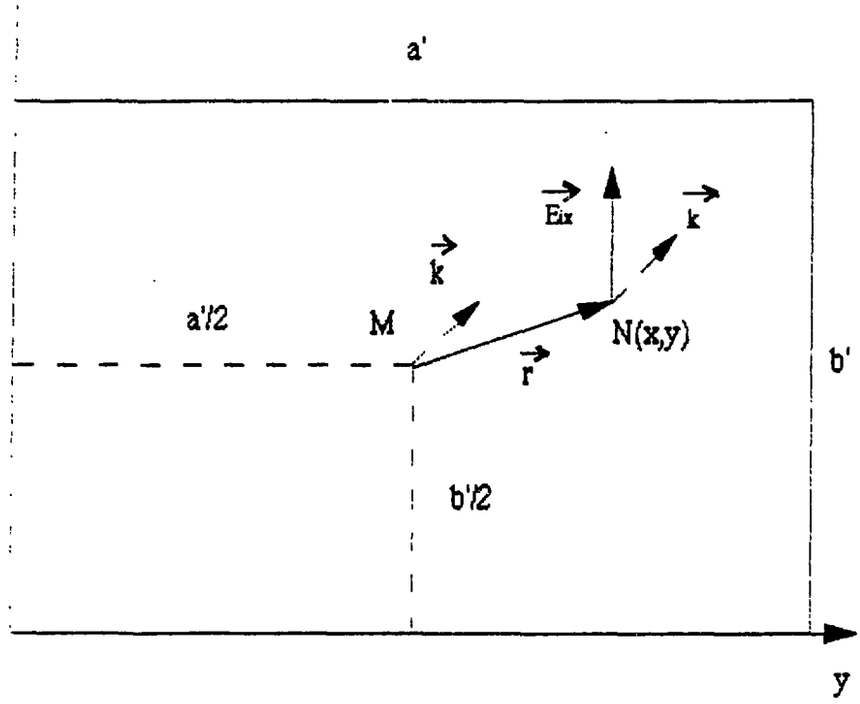

Fig 11

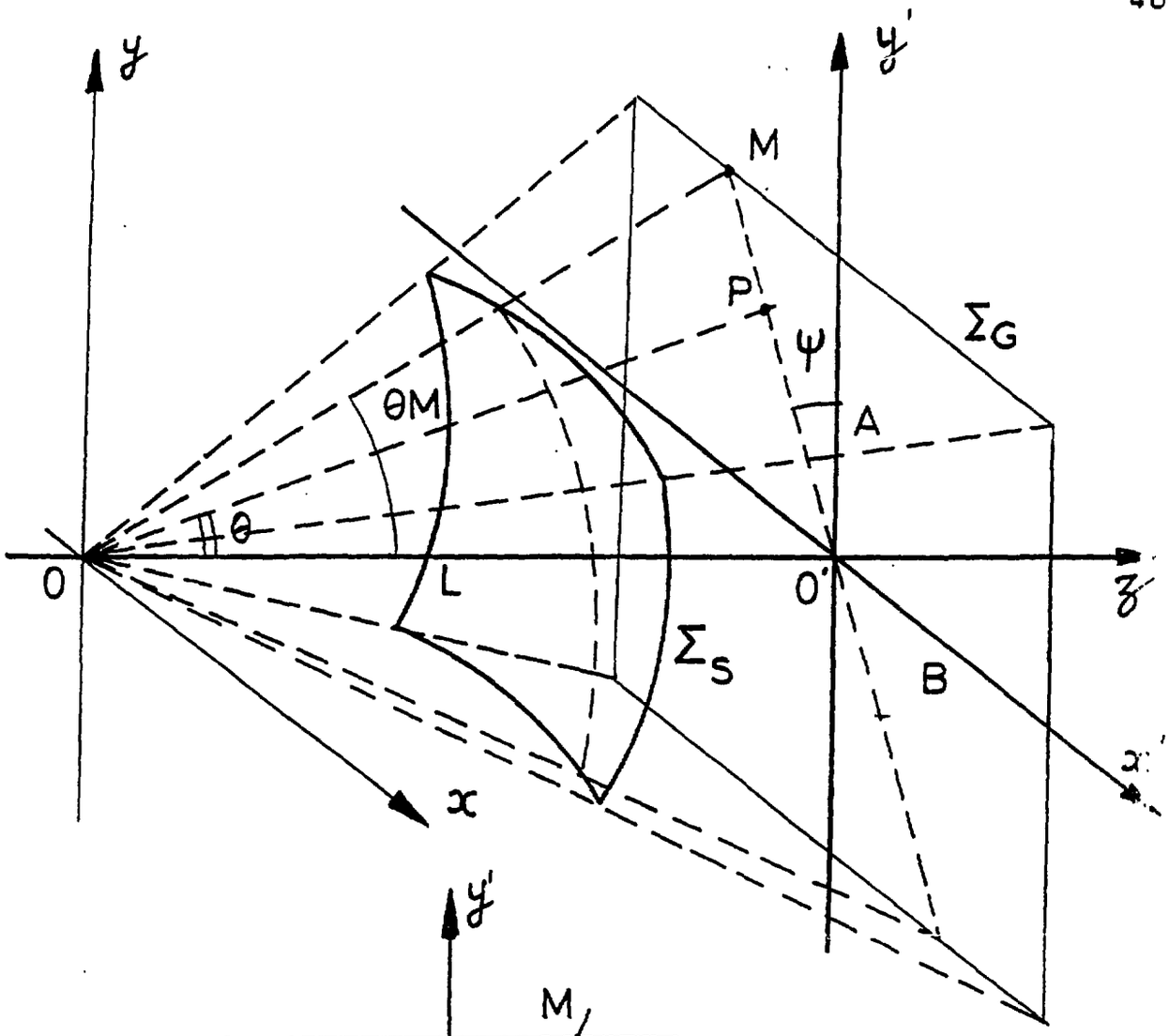

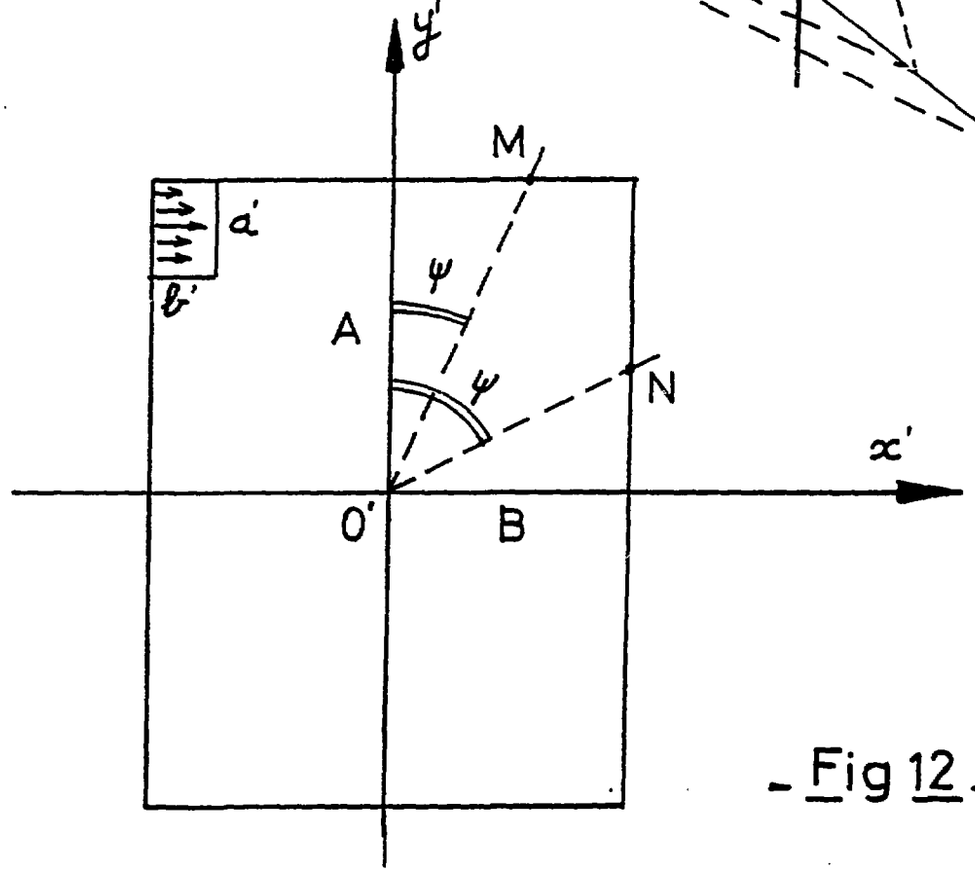

- Fig 12 -

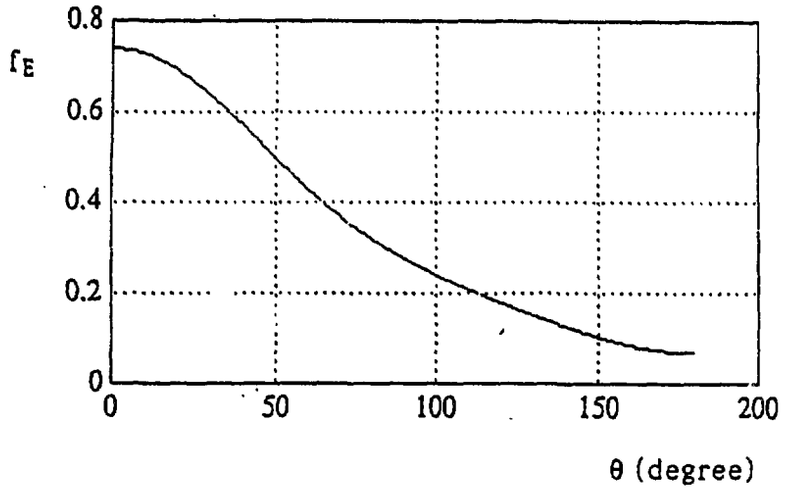

Fig (13) Far-field pattern $f_E(\theta)$ of the TE_{10} mode
in E plane f=3.7 GHz a=72.1 mm b=38 mm

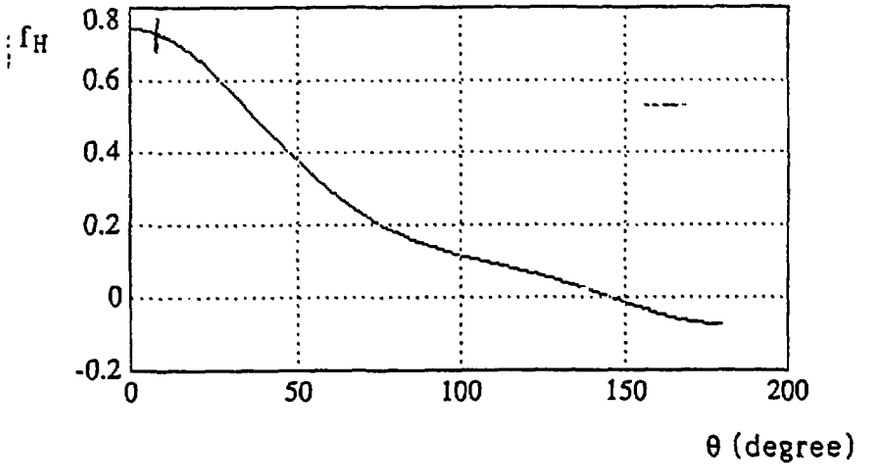

Fig (14) Far-field pattern $f_H(\theta)$ of the TE_{10} mode
in H plane f = 3.7 GHz a = 72.1 mm b = 38 mm

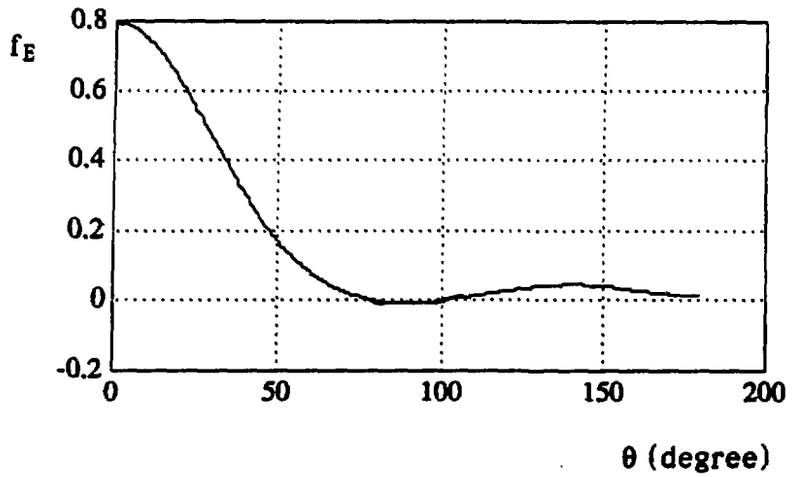

Fig (15) Far-field pattern $f_E(\theta)$ of the TE_{10} mode in E plane f=8 GHz a=72.1 mm b=38 mm

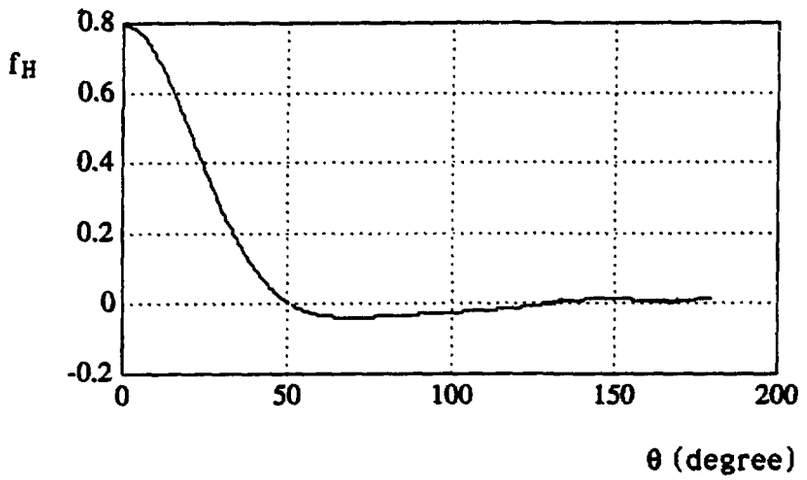

Fig (16) Far-field pattern $f_H(\theta)$ of the TE_{10} mode in H plane f=8 GHz a=72.1 mm b=38 mm

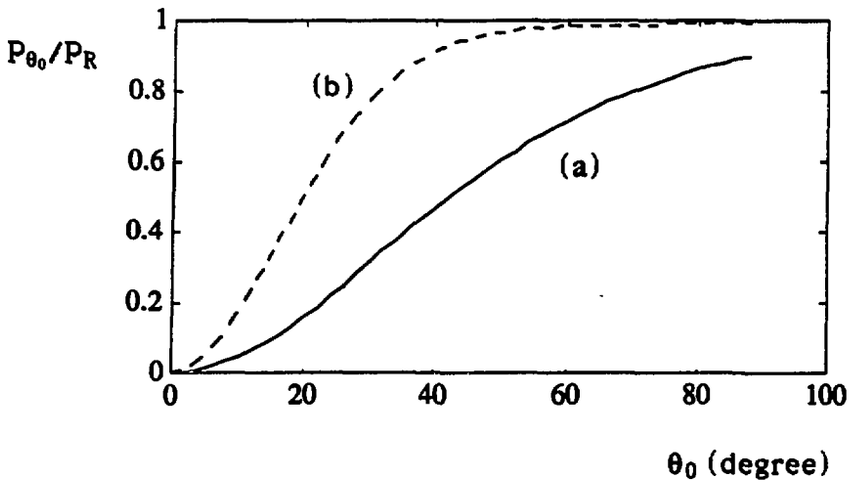

Fig (17) Normalized power P_{θ_0}/P_R within angle θ_0
a = 72.1 mm b = 38 mm (a) f = 3.7 GHz (b) f = 8 GHz

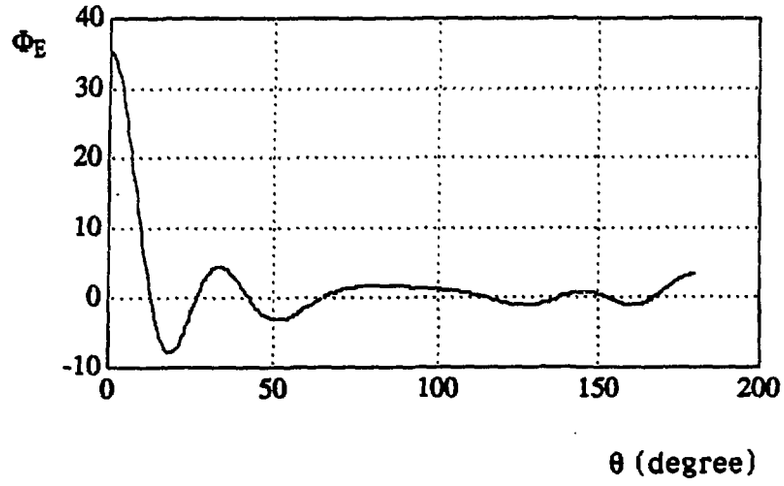

Fig (18) Far-field pattern Φ_E of the RA in E plane
f=3.7 GHz a=72.1mm b=38 mm n_x=8 n_y=6

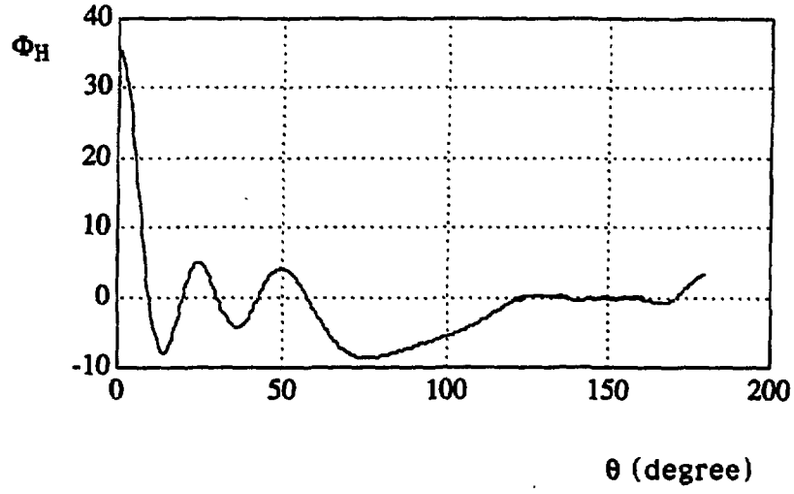

Fig (19) Far-field pattern Φ_H of the RA in H plane
f=3.7 GHz a=72.1mm b=38 mm n_x=8 n_y=6

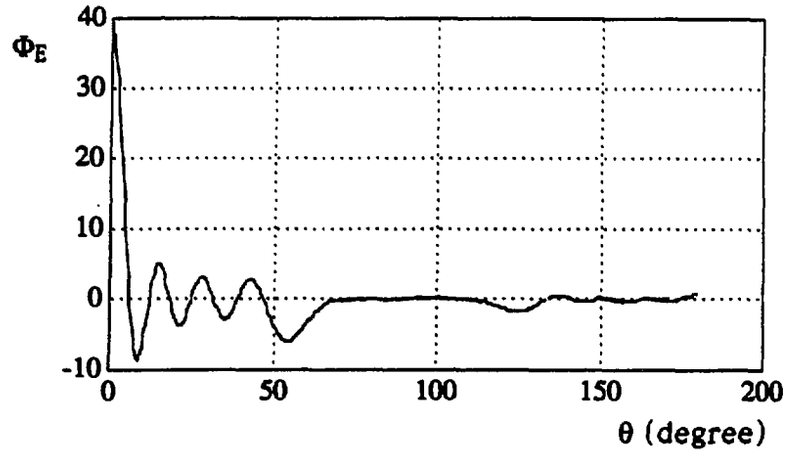

Fig (20) Far-field pattern $\Phi_E(\theta)$ of the RA in E plane
f=8 GHz a=72.1mm b=38 mm n_x=8 n_y=6

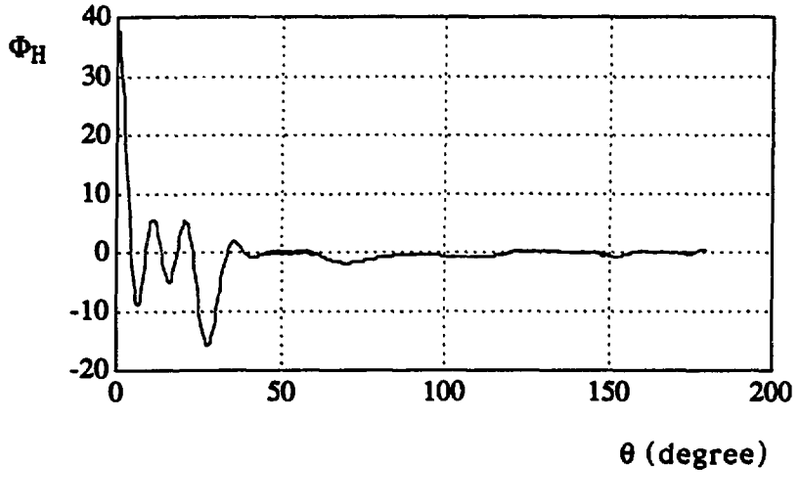

Fig (21) Far-field pattern $\Phi_H(\theta)$ of the RA in H plane
f=8 GHz a=72.1mm b=38 mm n_x=8 n_y=6

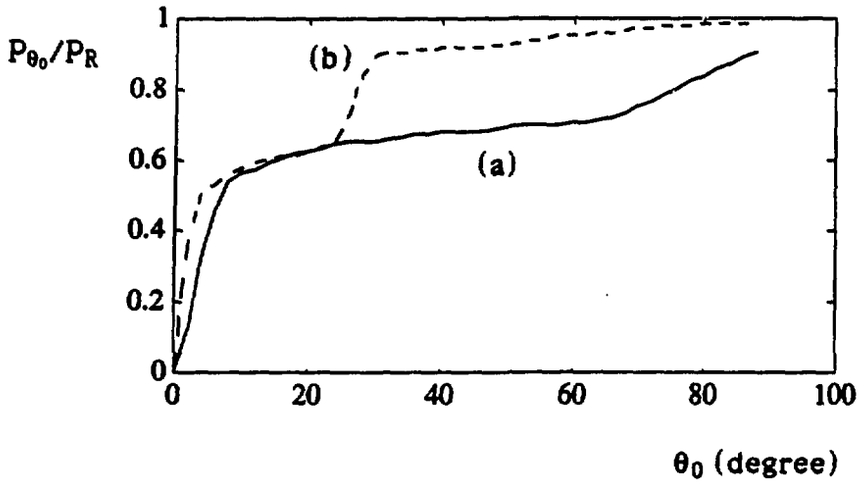

Fig (22) Normalized power P_{θ_0}/P_R within angle θ_0
a = 72.1 mm b = 38 mm n_x = 8 n_y = 6 d_x = 22.5 mm
d_y = 40 mm (a) f = 3.7 GHz (b) f = 8 GHz

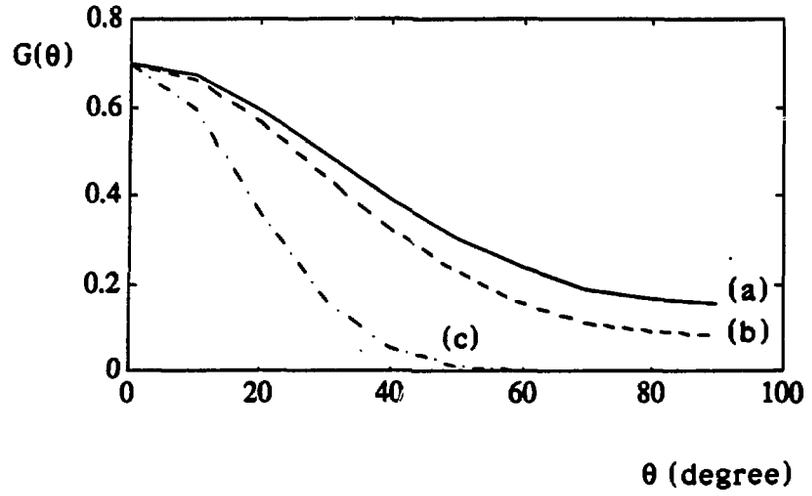

Fig (23) Coupling coefficient G(θ)
a = 72.1 mm b = 38 mm f=3.7 GHz
(a) ψ=0 degree (b) ψ=45 degree (c) ψ=90 degree

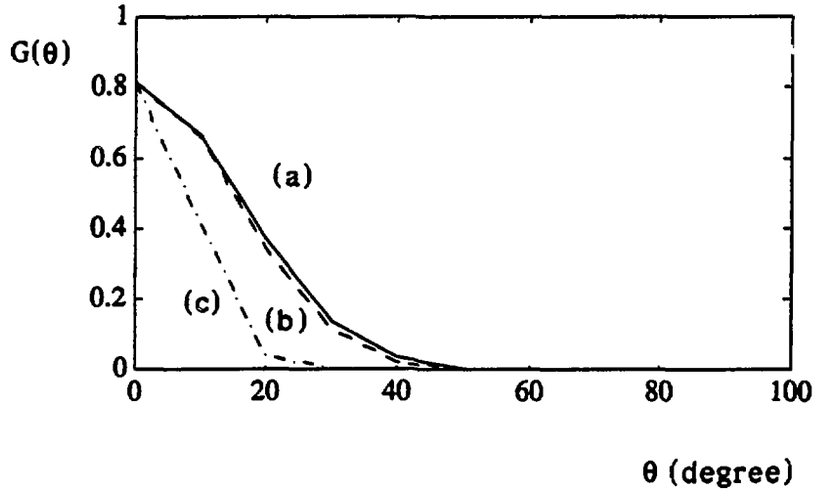

Fig (24) Coupling coefficient G(θ)
a = 72.1 mm b = 38 mm f=8 GHz
(a) ψ=0 degree (b) ψ=45 degree (c) ψ=90 degree

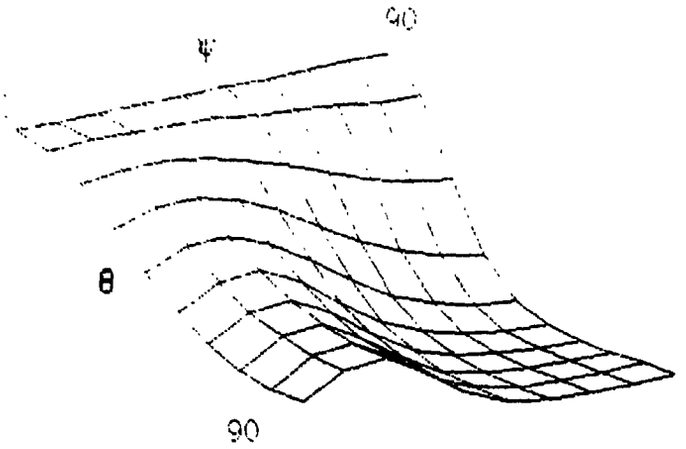

Fig (25) Space representation of $G(\theta,\psi)$
f=3.7 GHz a=72.1 mm b=38 mm

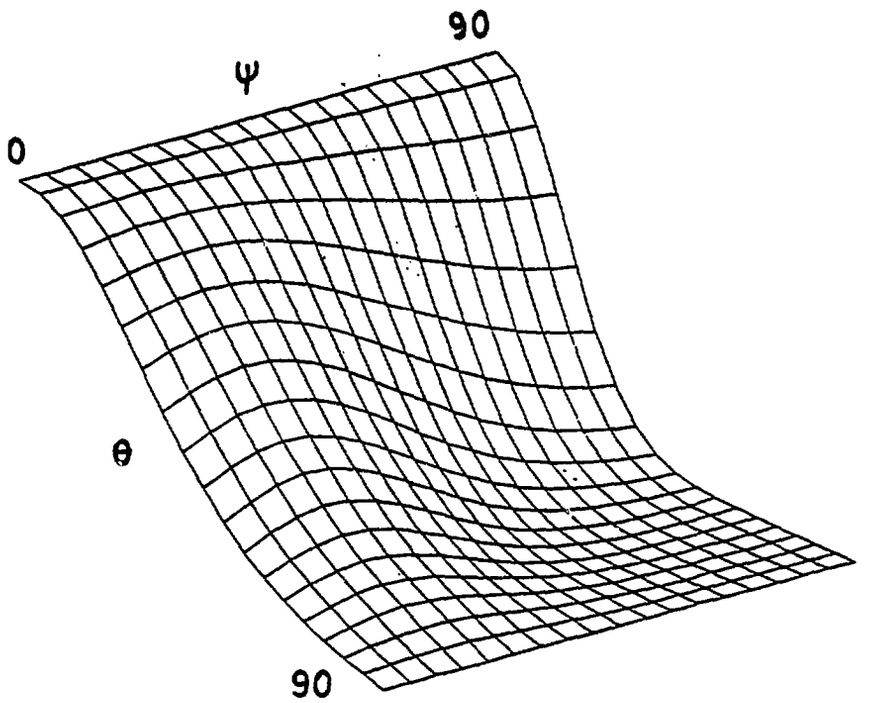

Fig (26) Space representation of $G(\theta,\psi)$
f = 8 GHz a =72.1 mm b = 38 mm

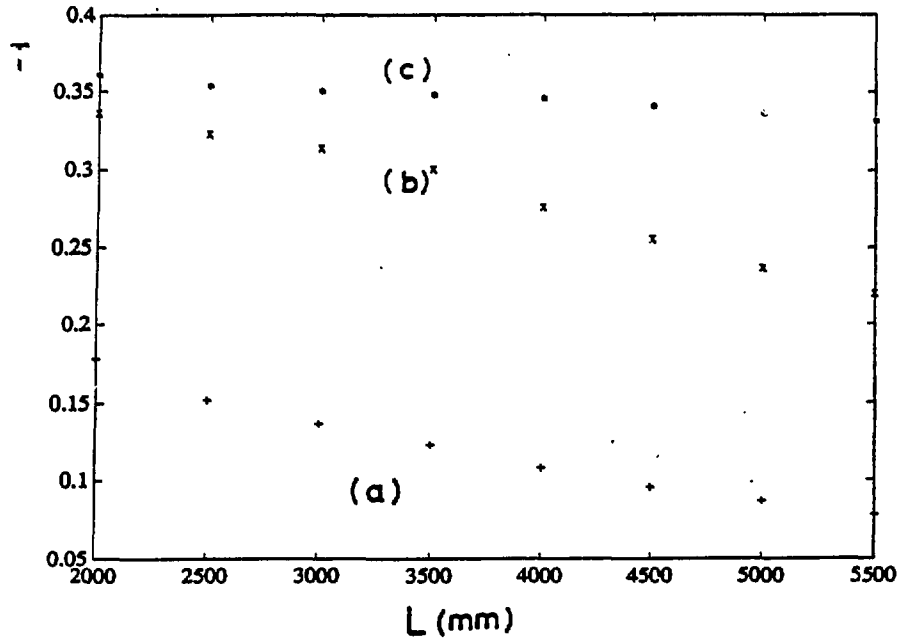

Fig (27) Power transmission T
f=3.7 GHz d_x=22.5 mm d_y=40 mm
a=72.1 mm b=38 mm n_x=8 n_y=6 Γ=0
(a) 2A=938 mm 2B=456 mm
(b) 2A=1876 mm 2B=912 mm
(c) 2A=3752 mm 2B=1824 mm

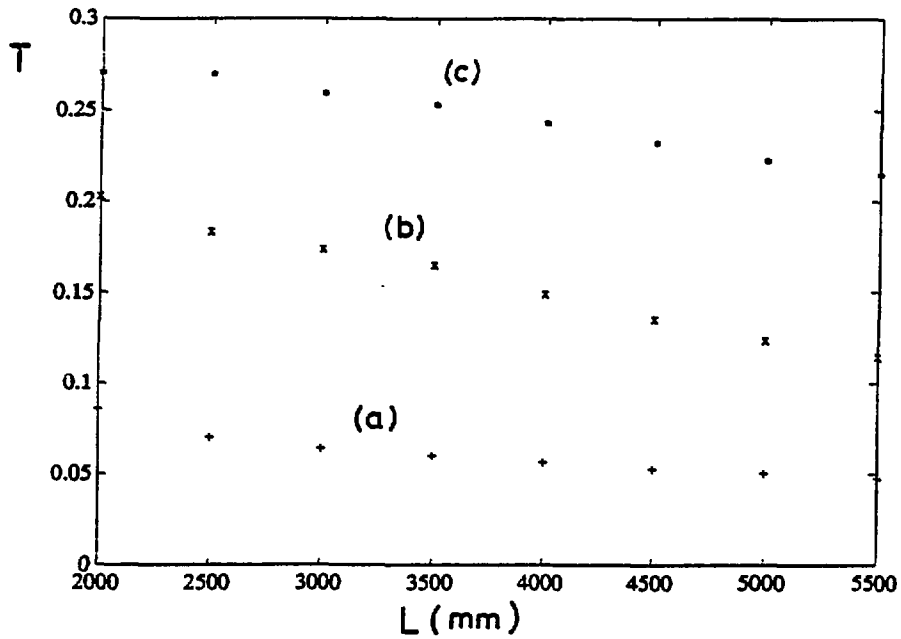

Fig (28) Power transmission T
f=8 GHz d_x=22.5 mm d_y=40 mm
a=72.1 mm b=38 mm n_x=8 n_y=6 Γ=0
(a) 2A=938 mm 2B=456 mm
(b) 2A=1876 mm 2B=912 mm
(c) 2A=3752 mm 2B=1824 mm

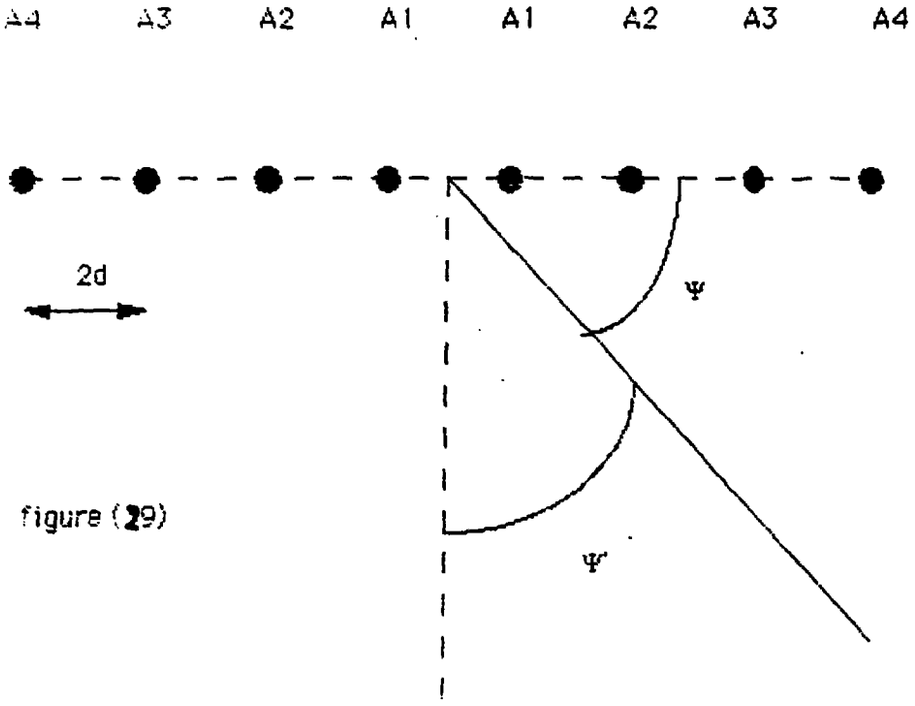

figure (29)

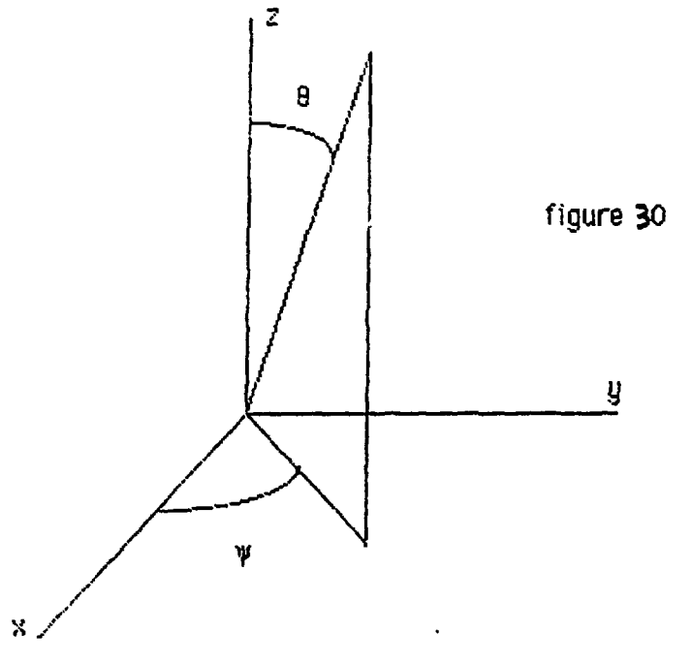

figure 30

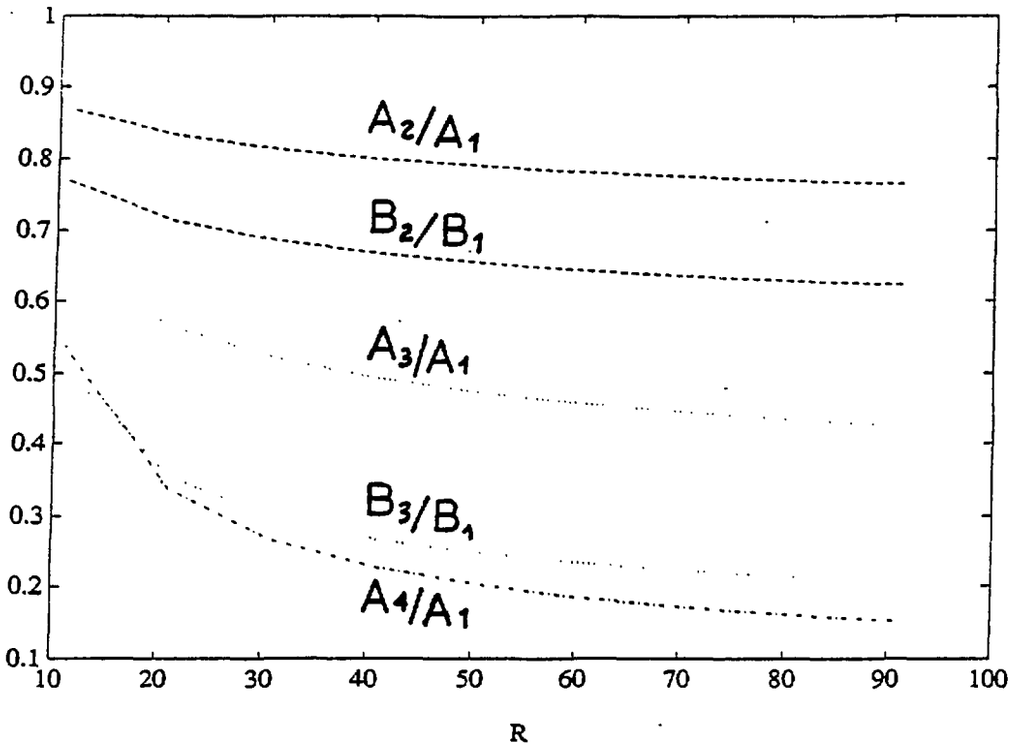

Fig(31) Ratio of the amplitudes of 8 A (resp 6 B) equally spaced and symmetrically fed sources compared to the central one A_1 (resp B_1) depending on the ratio R of the main lobe vs the first secondary one

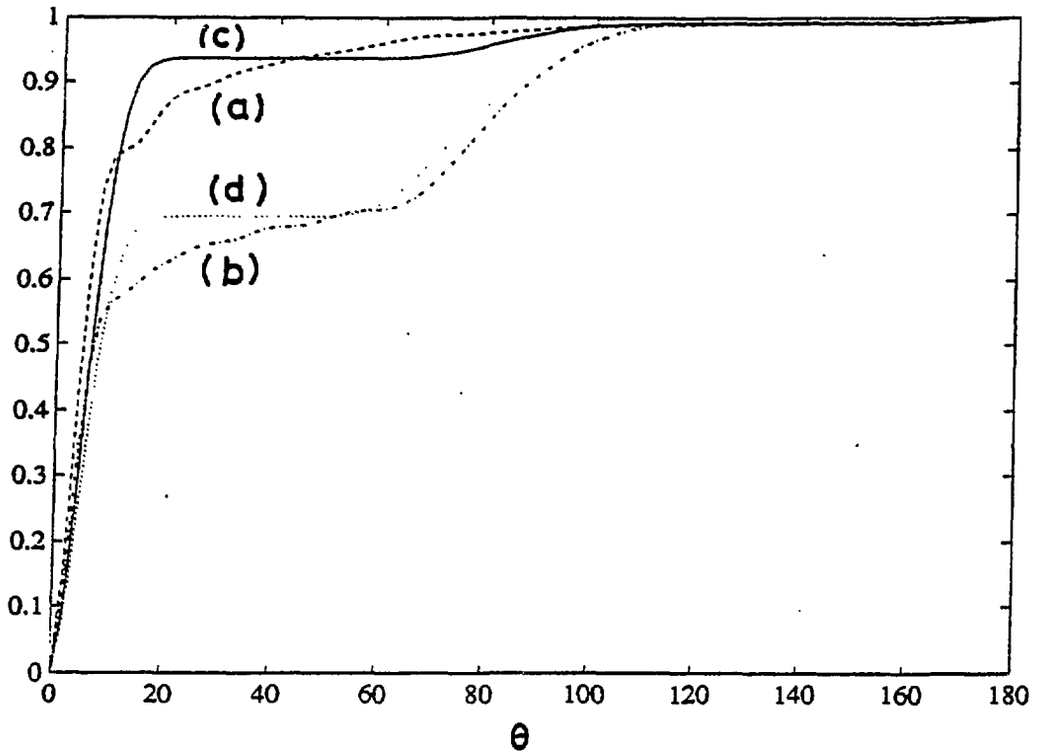

Fig (32) Normalized power $\frac{P_{\theta_0}}{P_R}$ within angle θ_0

f=3.7 GHz a=72.1 mm b=38 mm n_x=8 n_y=6 d_x=22.5 mm

Equally fed sources (a) d_y=35 mm (b) d_y=40 mm

(c) d_y=35 mm (d) d_y=40 mm

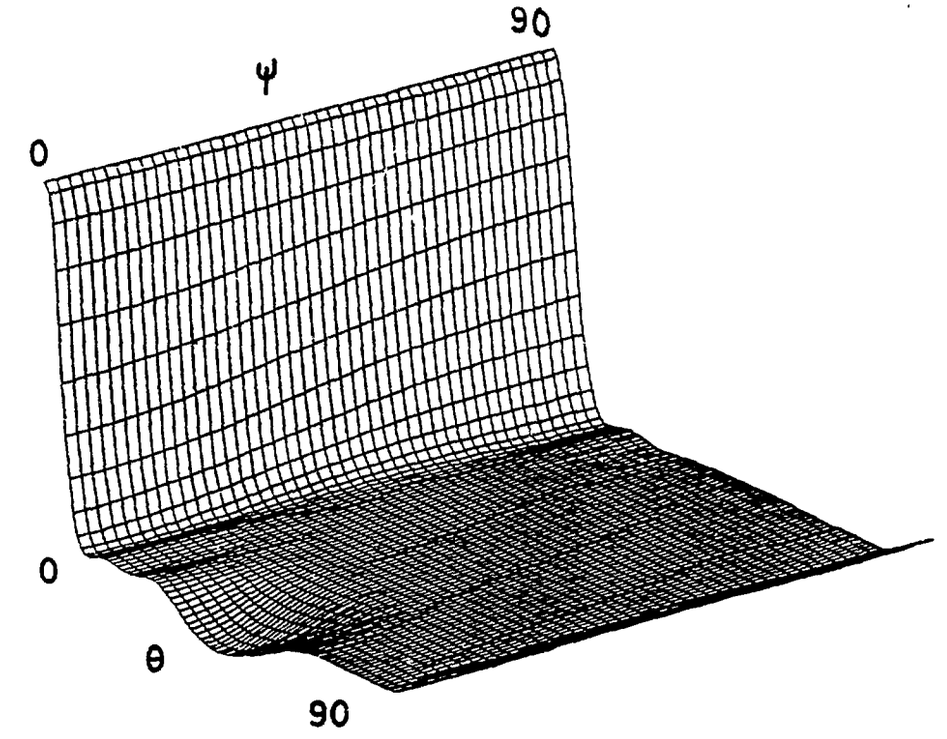

fig(33) Far-field pattern of RA when each waveguide is fed with an amplitude different computed by Dolph method . f=3.7GHz a=72.1 mm b=38 mm
d_x=40 mm d_y=35 mm

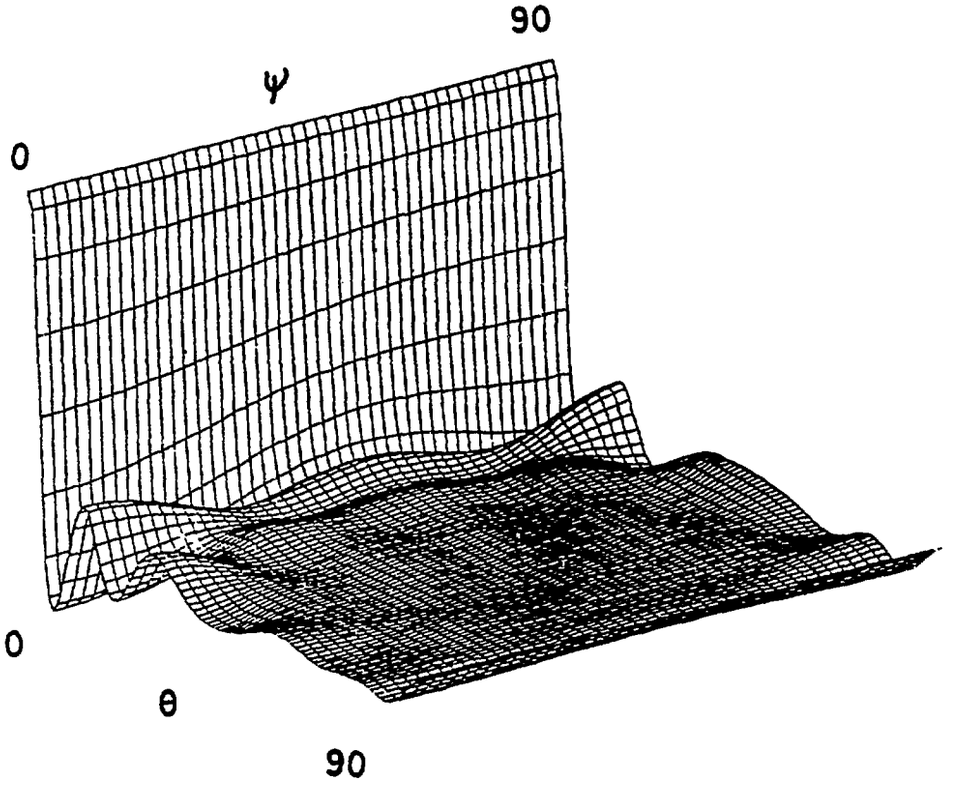

fig(34) Far-field pattern of RA when each waveguide is fed with the same amplitude
f=3.7GHz a=72.1 mm b=38 mm
d_x=40 mm d_y=35 mm

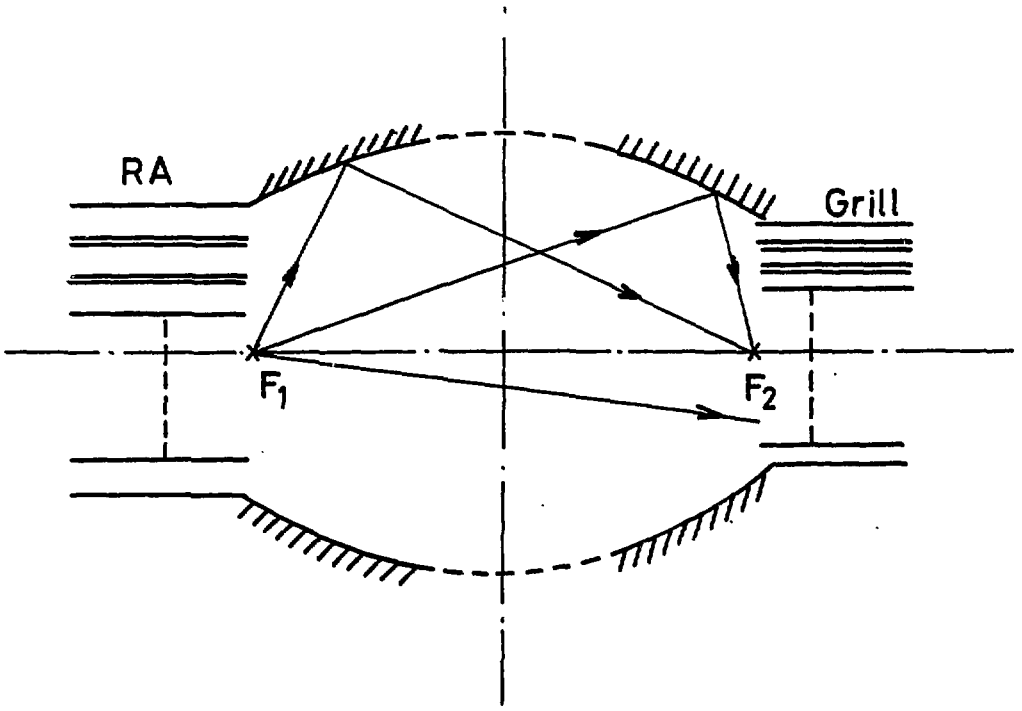

Fig 35

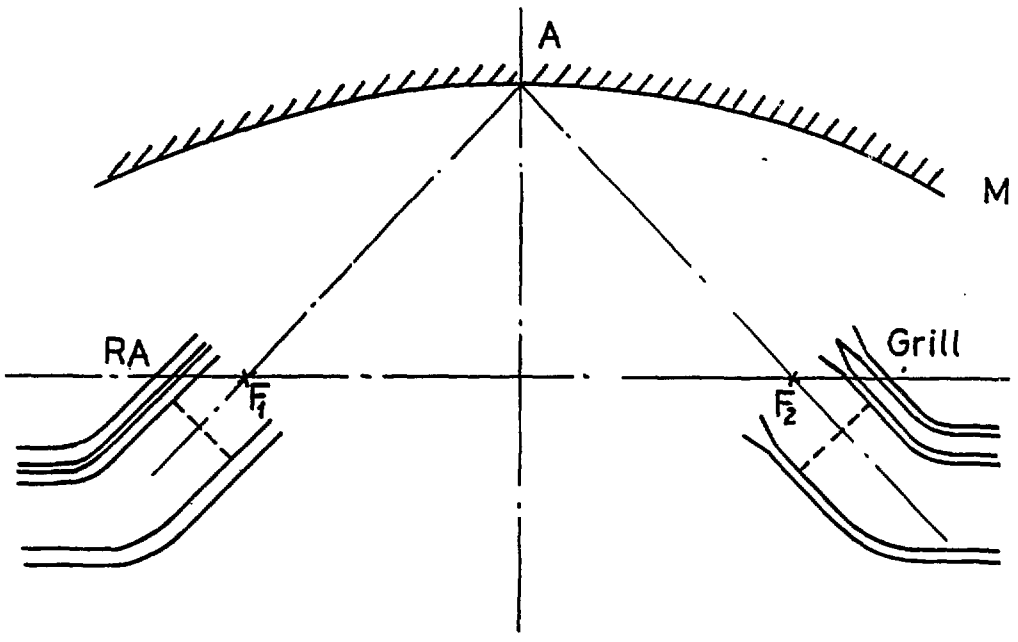

Fig 36

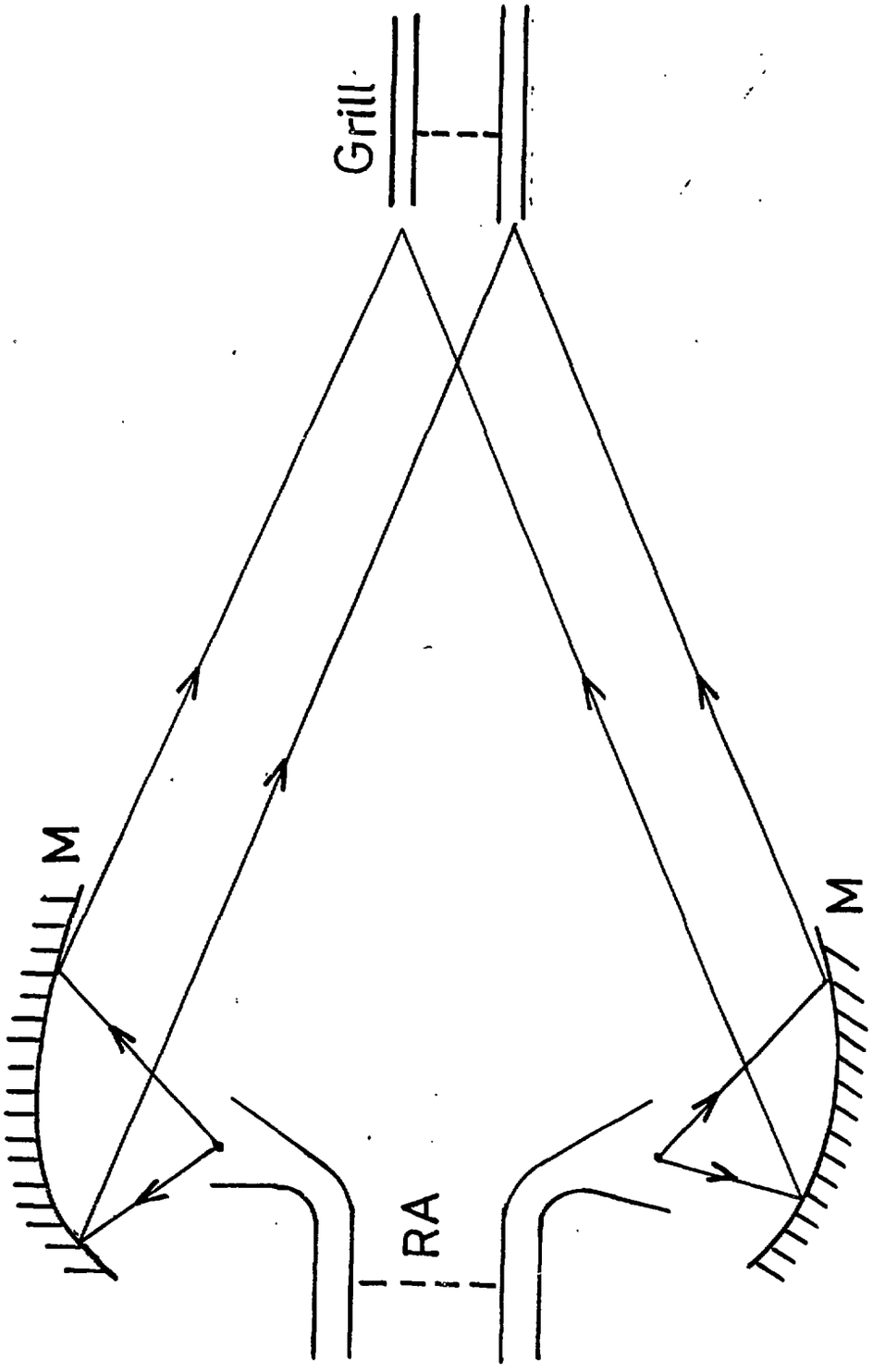

- Fig 37 -

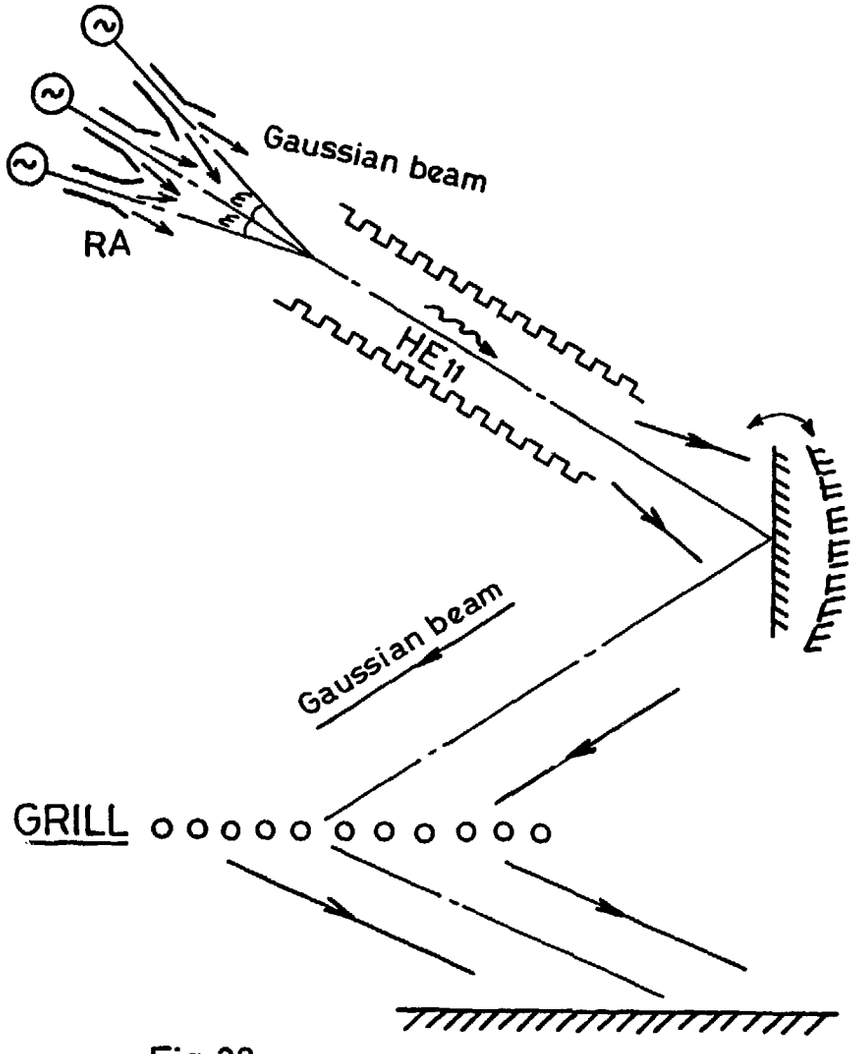
Gaussian beam
RA
HE11
Gaussian beam
GRILL
Plasma

Fig 38

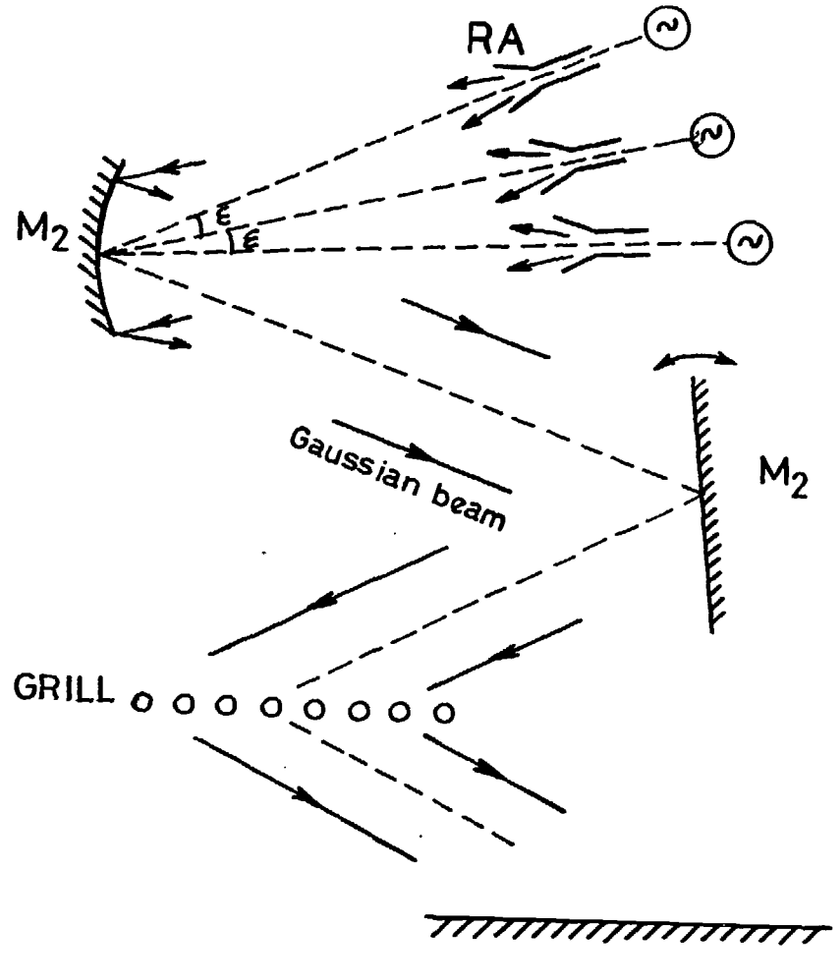
RA
M2
Gaussian beam
M2
GRILL
Plasma

Fig 39

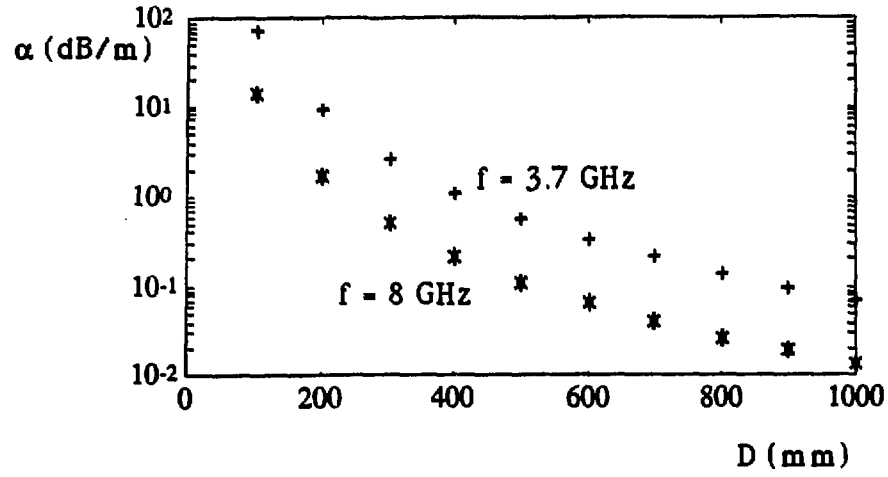

Fig (40) Attenuation of waveguide with optimal material wall HE_{11} mode

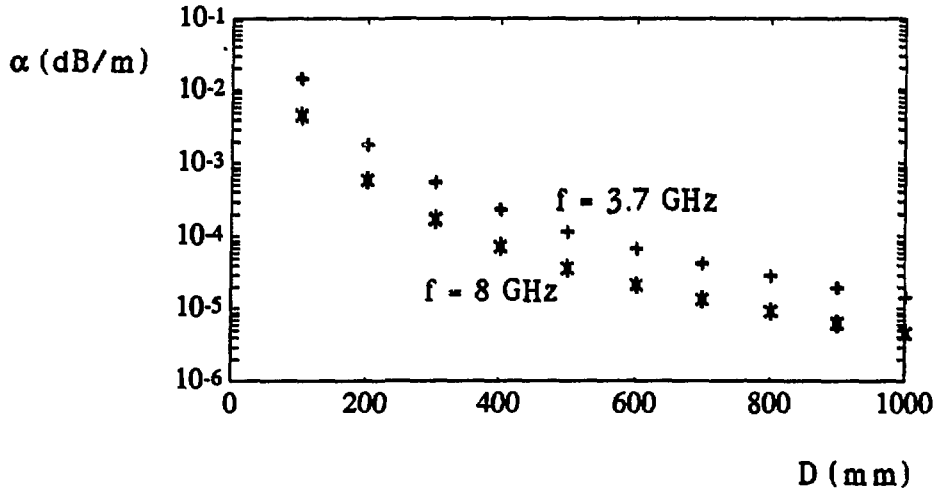

Fig (42) Attenuation of dielectric lined waveguide HE_{11} mode

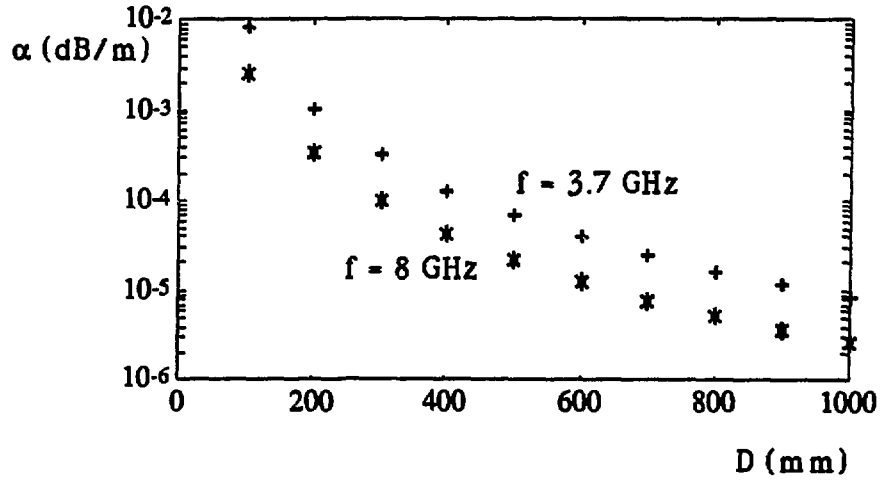

Fig (44) Attenuation of corrugated waveguide HE_{11} mode

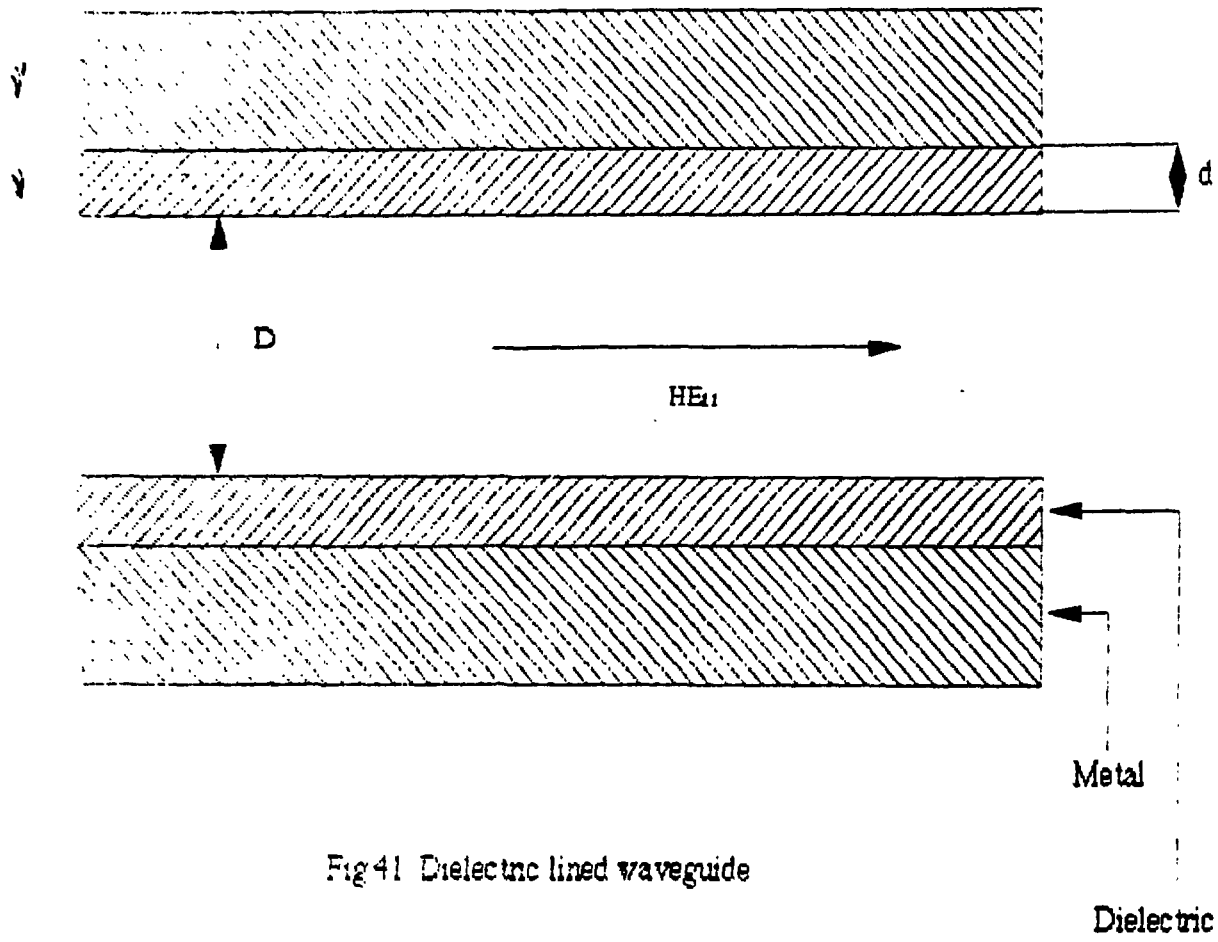

Fig 41 Dielectric lined waveguide

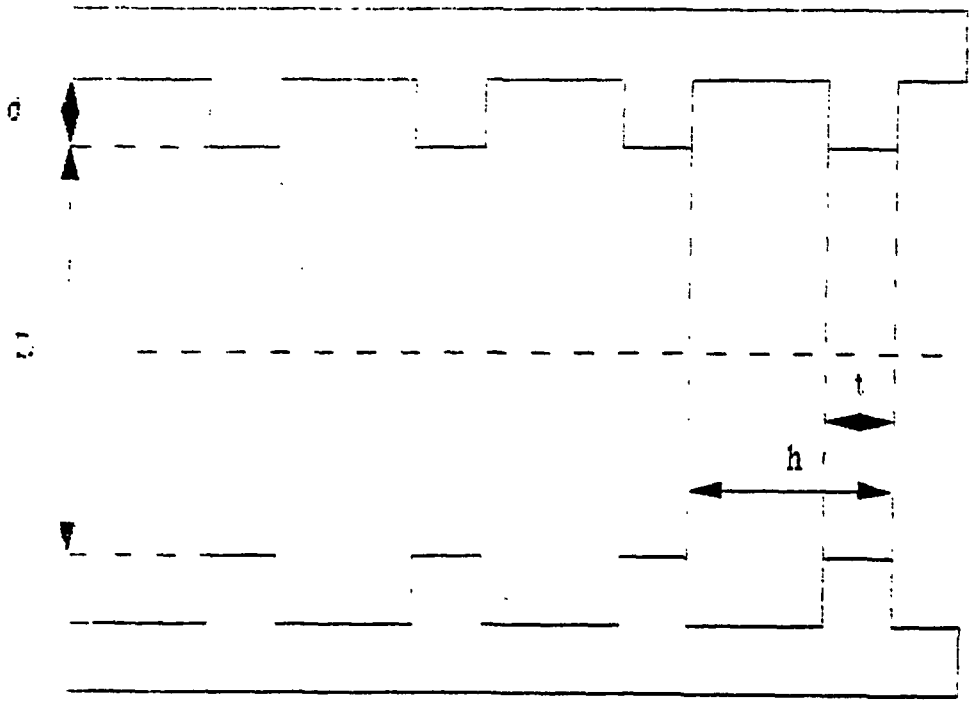

Fig(43) Metallic corrugated waveguide

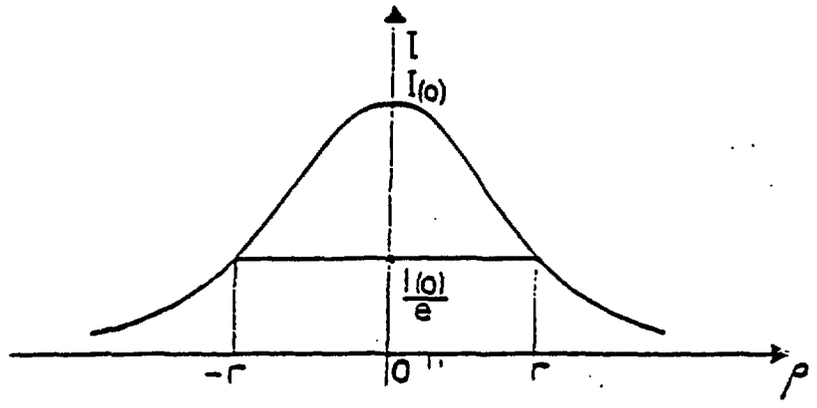

Fig 45 *Gaussian beam intensity in a cross section plane*

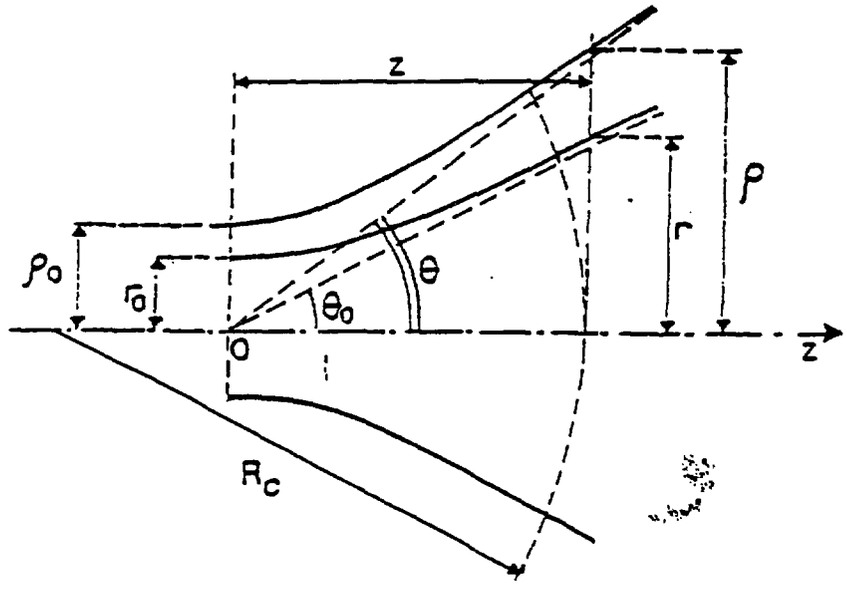

Fig 46 *Main parameters of a Gaussian beam*

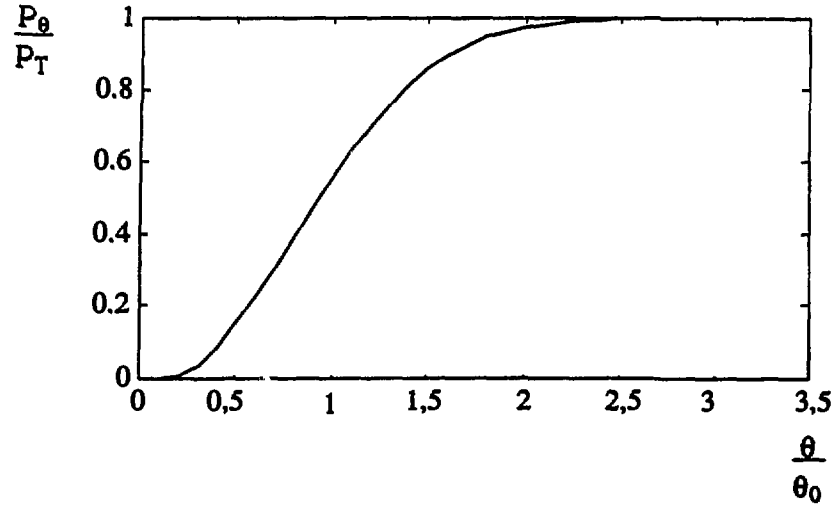

Fig (47) Normalized beam power within angle θ

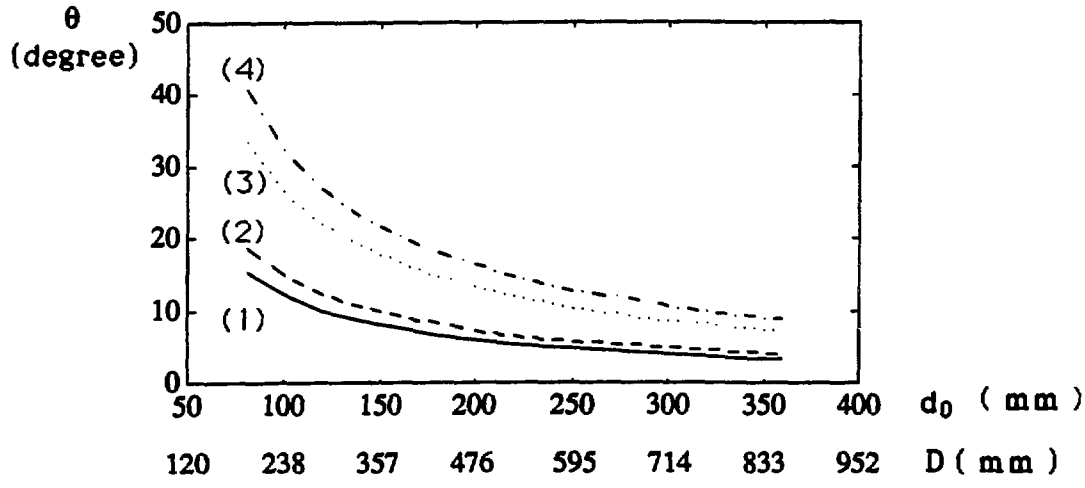

(1) f = 8 GHz Pθ/PT -0.96

(2) f = 8 GHz Pθ/PT -0.99

(3) f=3.7 GHz Pθ/PT-0.96

(4) f=3.7 GHz Pθ/PT-0.99

Fig 48